

EFFECTS OF SYNTHESIS AND DOPING METHODS ON
THERMOLUMINESCENCE GLOW CURVES OF MANGANESE DOPED
LITHIUM TETRABORATE

A THESIS SUBMITTED TO
THE GRADUATE SCHOOL OF NATURAL AND APPLIED SCIENCES
OF
MIDDLE EAST TECHNICAL UNIVERSITY

BY

MEHMET KAYHAN

IN PARTIAL FULFILLMENT OF THE REQUIREMENTS
FOR
THE DEGREE OF MASTER OF SCIENCE
IN
CHEMISTRY

JUNE 2009

Approval of the thesis:

EFFECTS OF SYNTHESIS AND DOPING METHODS ON
THERMOLUMINESCENCE GLOW CURVES OF MANGANESE DOPED
LITHIUM TETRABORATE

submitted by **MEHMET KAYHAN** in partial fulfillment of the requirements for the
degree of **Master of Science in Chemistry Department, Middle East Technical
University** by,

Prof. Dr. Canan Özgen
Dean, Graduate School of **Natural and Applied Sciences**

Prof. Dr. Ahmet M. Önal
Head of Department, **Chemistry**

Assoc. Prof. Dr. Ayşen Yılmaz
Supervisor, **Chemistry Dept., METU**

Examining Committee Members:

Prof. Dr. Gülhan Özbayoğlu
Mining Engineering Dept., METU

Assoc. Prof. Dr. Ayşen Yılmaz
Chemistry Dept., METU

Prof. Dr. Ceyhan Kayran
Chemistry Dept., METU

Prof. Dr. Ali Usanmaz
Chemistry Dept., METU

Prof. Dr. Deniz Üner
Chemical Engineering Dept., METU

Date:

I hereby declare that all information in this document has been obtained and presented in accordance with academic rules and ethical conduct. I also declare that, as required by these rules and conduct, I have fully cited and referenced all material and results that are not original to this work.

Name, Last Name : Mehmet Kayhan

Signature :

ABSTRACT

EFFECTS OF SYNTHESIS AND DOPING METHODS ON THERMOLUMINESCENCE GLOW CURVES OF MANGANESE DOPED LITHIUM TETRABORATE

Kayhan, Mehmet

M. Sc., Department of Chemistry

Supervisor: Assoc. Prof. Dr. Ayşen Yılmaz

June 2009, 59 Pages

Thermoluminescence dosimetry is an interesting research area for over the few past decades, especially in the fields of environmental, personnel, and clinical radiation applications. Even though, for a long time many thermoluminescent (TL) materials are being used in radiation dosimetry, the topic is open for extensive research to get new TL materials having lower cost or better performance.

Lithium tetraborate ($\text{Li}_2\text{B}_4\text{O}_7$, LTB) is one of the most promising materials for dosimetric applications with its tissue equivalent effective nuclear charge. Many researchers investigated the TL properties of LTB doped with different activators such as: Mn, Cu, Ag, and Mg.

In this study, differences in glow curves of Mn doped LTB powder samples synthesized with solid and wet synthesis methods and doped by using solid and wet

doping techniques were investigated. Firstly, LTB was synthesized by using wet synthesis method which mainly comprises dissolution of reactants in water as solvent. Second way to produce LTB which was used in this study was solid synthesis method. In solid synthesis method, reactants were mixed in powder form.

In the second part of the study, LTB produced by two different methods were doped with Mn and additionally Ag, Mg or P by using two different doping techniques.

In order to see structural differences between differently synthesized and differently doped LTB samples which contained different amount of dopant powder X-Ray Diffraction (XRD) method was employed. Besides, FTIR (Fourier Transform Infrared) spectroscopy analyses were performed in order to detect differences in the bond structure caused by doping. Additionally, Inductively Coupled Plasma Optical Emission Spectrometer (ICP-OES) was used to determine the actual amount of dopant in LTB. Also morphological structures of samples were compared by using Scanning Electron Microscopy (SEM). Thermoluminescence measurements were performed with (TLD) Thermoluminescence Dosimeter equipment.

XRD and FTIR analysis showed that syntheses of products were done in well success. Addition of dopants did not cause any changes in structural or bonding properties of LTB. It was possible to observe that, synthesis and doping methods and dopant concentration effect the thermoluminescence glow curves of doped LTB.

Keywords: Lithium tetraborate, inorganic synthesis methods, material characterization techniques, thermoluminescence

ÖZ

MANGAN KATKILANMIŞ LİTYUM TETRABORATIN SENTEZ VE KATKILAMA YONTEMLERİNİN ISISAL IŞILDAMA EĞRİSİ ÜZERİNE ETKİLERİ

Kayhan, Mehmet

Yüksek Lisans, Kimya Bölümü

Tez Yöneticisi: Doç. Dr. Ayşen Yılmaz

Haziran 2009, 59 Sayfa

Isısal ışıldama dozimetresi özellikle çevre, personel ve klinik radyasyon uygulamalarında, son yıllarda ilgi çeken bir araştırma konusudur. Isısal ışıldayan (TL) malzemeler uzun zamandır radyasyon dozimetresinde kullanılmasına karşın konu halen yeni, düşük maliyetli veya daha yüksek performanslı malzemeler elde etmek için detaylı araştırmaya açıktır.

Lityum tetraborat ($\text{Li}_2\text{B}_4\text{O}_7$, LTB) doku eşdeğer etkin çekirdek yükü değeriyle dozimetrik uygulamalar için en çok umut vadeden malzemelerden biridir. Birçok araştırmacı Mn, Cu, Ag ve Mg gibi değişik etkinleştiriciler ile katkılanmış LTB'nin TL özelliklerini araştırmıştır.

Bu çalışmada katı ve ıslak sentez yöntemleriyle sentezlenmiş ve katı ve ıslak katkılama teknikleriyle Mn katkılanmış LTB toz numunelerinin ışına eğrilerindeki farklılıklar incelenmiştir. İlk olarak LTB, temel olarak giriş malzemelerinin suda çözünmesini içeren ıslak sentez yöntemi kullanılarak sentezlenmiştir. LTB üretiminin diğer bir yolu olarak bu çalışmada kullanılan yol katı sentez yöntemidir. Katı sentez yönteminde giriş malzemeleri toz halde karıştırılmıştır.

Bu araştırmanın ikinci kısmında iki değişik yöntemle sentezlenen LTB, iki farklı teknik kullanılarak Mn ve ilaveten Ag, Mg veya P ile katkılanmıştır.

Değişik sentez ve katkılama yöntemleriyle elde edilmiş, değişik miktarlarda katkı içeren LTB örnekleri arasındaki yapısal değişiklikleri görmek için toz x-ışını kırınımı (XRD) yöntemi uygulanmıştır. Bunun yanı sıra, katkılamadan kaynaklanan, bağ yapısındaki değişiklikleri tespit etmek için, FTIR spektrometresi analizleri yapılmıştır. LTB içerisindeki katkının gerçek miktarının tespiti için Endüktif Eşleşmiş Plazma Optik Emisyon Spektrometresi (ICP-OES) kullanılmıştır. Ayrıca örneklerin morfolojik yapıları taramalı elektron mikroskobu (SEM) ile karşılaştırılmıştır. Isısal ışıldaama ölçümleri, ısısal ışıldaama dozimetresi (TLD) cihazı kullanılarak yapılmıştır.

XRD ve FTIR analizleri ürünlerin başarıyla sentezlendiğini göstermiştir. Katkı malzemelerinin eklenmesi LTB'nin yapısal veya bağ özelliklerinin değişimine sebep olmamıştır. Sentez ve katkılama yöntemlerinin ve katkı malzemesi konsantrasyonunun, katkılanmış LTB'nin termoluminesans ışına eğrilerini etkilediği görülmüştür.

Anahtar Sözcükler: Lityum tetraborat, anorganik sentez yöntemleri, madde karakterizasyon, ısısal ışıldaama

*To my wife Emine and my parents Yakup and
Seviye*

ACKNOWLEDGEMENTS

I would like to extend my gratitude to;

... Associate Prof. Dr. Ayşen Yılmaz for her encouragement and supervision throughout my studies...

... my group members Semih Seyyidođlu, Tolga Depçi, Esin Pekpak, and Levent İlkay for their help and support...

... Past and present members of Chemistry Department; where I learned a lot and made great friends during the last 2 years...

... my friend Abidin Balan for his encouragement and invaluable friendship...

... my parents; Yakup and Seviye and my sister Hatice for their continuous support and help...

I want to also specially thank my wife Emine for her endless support and love.

TABLE OF CONTENTS

ABSTRACT	iv
ÖZ	vi
ACKNOWLEDGEMENTS	ix
TABLE OF CONTENTS	x
LIST OF TABLES	xv
LIST OF FIGURES	xvi
CHAPTER 1	1
INTRODUCTION	1
1.1 THERMOLUMINESCENCE	1
1.1.1 THEORY OF THERMOLUMINESCENCE.....	2
1.1.1.1 Trapping.....	3
1.1.1.2 Recombination.....	4
1.1.2 APPLICATIONS OF THERMOLUMINESCENCE	5

1.1.2.1	Radiation dosimetry	5
1.1.2.1.1	Dosimetry applications	5
1.1.2.1.1.1	Personnel dosimetry	5
1.1.2.1.1.2	Environmental dosimetry	5
1.1.2.1.1.3	Medical dosimetry	6
1.1.2.1.1.4	Retrospective dosimetry	6
1.1.2.1.1.5	High dose	6
1.1.2.2	TL dating of archeological and geological samples	7
1.1.3	THERMOLUMINESCENCE DOSIMETRY	7
1.1.3.1	Properties of a TLD	7
1.1.3.2	Glow Curve	8
1.1.3.3	Dosimetric Peak	8
1.1.3.4	Error sources in TLD measurements	8
1.1.3.5	Dosimeter's Background	10
1.1.3.6	Annealing	10

1.1.3.7	The Effects of Heating Rate on TL Results.....	11
1.2	LITHIUM TETRABORATE.....	12
1.2.1	Physical Properties and Uses of LTB	12
1.2.2	Crystal structure of LTB	12
1.2.3	FTIR Spectrum of LTB	13
1.2.4	Synthesis of LTB	14
1.2.4.1	Polycrystalline LTB.....	14
1.2.4.2	LTB Thin Film.....	15
1.2.4.2.1	Solution preparation	15
1.2.4.2.2	Film preparation	16
1.2.4.3	Single Crystalline LTB.....	16
1.2.5	Doping of LTB with different metals	17
1.2.6	TL Studies on LTB in Literature.....	18
	OBJECTIVE	20
	CHAPTER 2	21

MATERIALS, EQUIPMENTS, AND METHODS.....	21
2.1 MATERIALS.....	21
2.2 EQUIPMENTS	21
2.2.1 Furnace.....	21
2.2.2 Powder X-Ray Diffractometer	21
2.2.3 Fourier Transform Infrared Spectrometer	22
2.2.4 Scanning Electron Microscope	22
2.2.5 Inductively Coupled Plasma Optical Emission Spectrometer	23
2.2.6 Thermoluminescence Reader	23
2.3 EXPERIMENTAL METHODS.....	23
2.3.1 Synthesis of LTB	23
2.3.1.1 Wet synthesis	24
2.3.1.2 High temperature solid state synthesis (solid synthesis)	24
2.3.2 Doping of metals into LTB	25
2.3.2.1 Wet doping method.....	27

2.3.2.2	Solid doping method.....	28
CHAPTER III		29
RESULTS AND DISCUSSIONS		29
3.1	Characterization	29
3.1.1	Powder X-Ray Diffraction (XRD).....	29
3.1.2	Inductively Coupled Plasma Optical Emission Spectrometer	37
3.1.3	Fourier Transform Infrared Spectroscopy (FTIR)	38
3.1.4	Scanning Electron Microscopy (SEM)	39
3.1.5	Thermoluminescence Dosimetry (TLD).....	41
CHAPTER IV		53
CONCLUSIONS.....		53
CHAPTER V.....		55
REFERENCES.....		55

LIST OF TABLES

Table 1: Luminescence phenomena and the methods of excitation.....	1
Table 2: Experiment chart for different synthesis and doping methods	26
Table 3: Experiment chart for co-doping studies.....	27
Table 4: X-ray analysis results for solid synthesized and 1 wt % Mn solid doped LTB.	33
Table 5: Observed d-spacing values for different samples, and theoretical d-spacing values for $\text{Li}_2\text{B}_4\text{O}_7$	34
Table 6: Observed d-spacing values for different samples containing different co-dopants, and theoretical d-spacing values for $\text{Li}_2\text{B}_4\text{O}_7$	35

LIST OF FIGURES

Figure 1: The three stages of thermoluminescence.....	3
Figure 2: Trapping of excited electrons upon exposure to radiation and recombination of trapped electrons upon external activation energy	4
Figure 3: Structure of the $\text{Li}_2\text{B}_4\text{O}_7$ lattice shown as projections of part of the tetragonal elementary cell along a [110]-type axis	13
Figure 4: FTIR spectrum of $\text{Li}_2\text{B}_4\text{O}_7\text{:Cu}$ sample at room temperature	14
Figure 5: XRD patterns of Wet synthesized undoped LTB (a), solid synthesized undoped LTB (b).....	30
Figure 6: XRD patterns of wet synthesized undoped LTB (a), solid synthesized undoped LTB (b), wet synthesized 1 wt % Mn wet doped LTB (c), wet synthesized 1 wt % Mn solid doped LTB (d), solid synthesized 1 wt % Mn wet doped LTB (e), and solid synthesized 1 wt % Mn solid doped LTB (f). Planes of LTB are shown on the top pattern.	31
Figure 7: Comparison of XRD patterns in varying Mn content	36
Figure 8: Problematic elements under Cu radiation.....	37
Figure 9: FTIR spectra of wet synthesized undoped LTB (a), solid synthesized undoped LTB (b), wet synthesized 1 wt % Mn wet doped LTB (c), wet synthesized 1	

wt % Mn solid doped LTB (d), solid synthesized 1 wt % Mn wet doped LTB (e), and solid synthesized 1 wt % Mn solid doped LTB (f). 38

Figure 10: SEM images of wet synthesized undoped LTB (A) and solid synthesized undoped LTB (B). 39

Figure 11: SEM images of wet synthesized 1 wt % Mn wet doped LTB (A), wet synthesized 1 wt % Mn solid doped LTB (B), solid synthesized 1 wt % Mn wet doped LTB (C), and solid synthesized 1 wt % Mn solid doped LTB (D). 40

Figure 12: SEM images of solid synthesized 1 wt % Mn 0.5 wt % Ag solid doped LTB (A), solid synthesized 1 wt % Mn 0.5 wt % P solid doped LTB (B), and solid synthesized 1 wt % Mn 0.5 wt % Mg solid doped LTB (C). 41

Figure 13: TL glow curves of undoped wet synthesized (a) and solid synthesized (b) LTB 42

Figure 14: TL glow curves of wet synthesized and Mn doped by wet doping method with varying Mn content from 0.1 wt % to 10 wt % 43

Figure 15: TL glow curves of wet synthesized and Mn doped by solid doping method with varying Mn content from 0.1 wt % to 10 wt % 44

Figure 16: TL glow curves of solid synthesized and Mn doped by wet doping method with varying Mn content from 0.1 wt % to 10 wt % 45

Figure 17: TL glow curves of solid synthesized and Mn doped by solid doping method with varying Mn content from 0.1 wt % to 10 wt % 46

Figure 18: Glow peak intensities of solid synthesized and solid doped LTB with varying Mn content.	47
Figure 19: Thermoluminescence measurements of wet synthesized 1 wt % Mn wet doped LTB (A), wet synthesized 1 wt % Mn solid doped LTB (B), solid synthesized 1 wt % Mn wet doped LTB (C), and solid synthesized 1 wt % Mn solid doped LTB (D).	48
Figure 20: TL glow curves of solid synthesized and Mn and Ag doped by solid doping method with varying Mn content from 0.1 wt % to 1 wt % for Mn and 0.5 wt % for Ag.	49
Figure 21: TL glow curves of solid synthesized and Mn and P doped by solid doping method with varying Mn content from 0.1 wt % to 1 wt % for Mn and 0.5 wt % for P.	50
Figure 22: TL glow curves of solid synthesized and Mn and Mg doped by solid doping method with varying Mn content from 0.1 wt % to 1 wt % for Mn and 0.5 wt % for Mg.	51
Figure 23: Thermoluminescence glow curves of LTB:Mn,Ag (A), LTB:Mn,P (B), and LTB:Mn,Mg (C).	52

CHAPTER 1

INTRODUCTION

1.1 THERMOLUMINESCENCE

The energy emitted as light by a material, which absorbed energy from an external source, when an electron goes back to its ground state energy level from excited higher energy level is called luminescence. Time passed between the absorption of external energy and the relaxation and emission of light is characteristic for materials. This characteristic time gives the opportunity of classification according to luminescence type. (S. W. S. McKeever, C. 1985) (R. Chen, S.W.S. McKeever, C. 1997) (R. Chen, Y. Kirsh, C. 1981)

Table 1: Luminescence phenomena and the methods of excitation. (C. Furetta, C. 2003)

LUMINESCENCE PHENOMENA	METHODS OF EXCITATION
Bioluminescence	Biochemical reactions
Cathodoluminescence	Electron beam
Chemiluminescence	Chemical reactions
Electroluminescence	Electric field
Photoluminescence	U.V. and infrared light
Piezoluminescence	Pressure (10 tons m^{-2})
Triboluminescence	Friction
Radioluminescence	Ionising radiation
Sonoluminescence	Sound waves
Fluorescence Phosphorescence Thermoluminescence Lyoluminescence	Ionizing radiation, U.V. and visible light

If this time is short enough (10^{-8} sec) for direct relaxation after excitation without any other extra processes, luminescence is called fluorescence. In fluorescence,

wavelength of the emitted light is larger than the wavelength of absorbed light since the energy is dispersed in the molecule.

If the time is larger than 10^{-4} sec, then this kind of luminescence is named as phosphorescence. In phosphorescence, time is a bit longer than in fluorescence since there is a metastable level which slows down the relaxation of excited electron by acting as a trap.

In the crystal structure of a molecule there may be imperfections (i.e., impurity atom lattice vacancy, dislocation) which traps electrons in conduction band of the material. These trapped excited electrons need activation energy to get rid of those traps and to go back to their ground state energy levels.

1.1.1 THEORY OF THERMOLUMINESCENCE

Thermoluminescence is the phenomenon of light emission from the charge carrier traps induced by activator impurities in an irradiated thermoluminescent (TL) material, when it is heated. (A. S. Pradhan, 1981) (A. T. Ege, 2007) Charge carriers are excited to traps, which are provided by impurities called dopants, give their extra energies as light while they are relaxing to their lower or ground states in heating process. Energy of heat helps the charge carriers to jump the activation barrier. The sensitivity of the detector is the amount of light released per unit of radiation dose. TL materials gives response as a glow curve with peaks when the trapped charge carriers are released. (J. Azorin, 1986) The position, size and shape of this glow curve (peak on the pattern of light output versus temperature) gives information about the X, gamma (γ) or beta (β) radiations stored in, with the characteristics of the material. Although the glow curve is influenced by the heating rate, radiation dose, and pre- and post-irradiation heat treatments, the emission spectrum mostly depends on the nature of the activator (A. T. Ege, 2007).

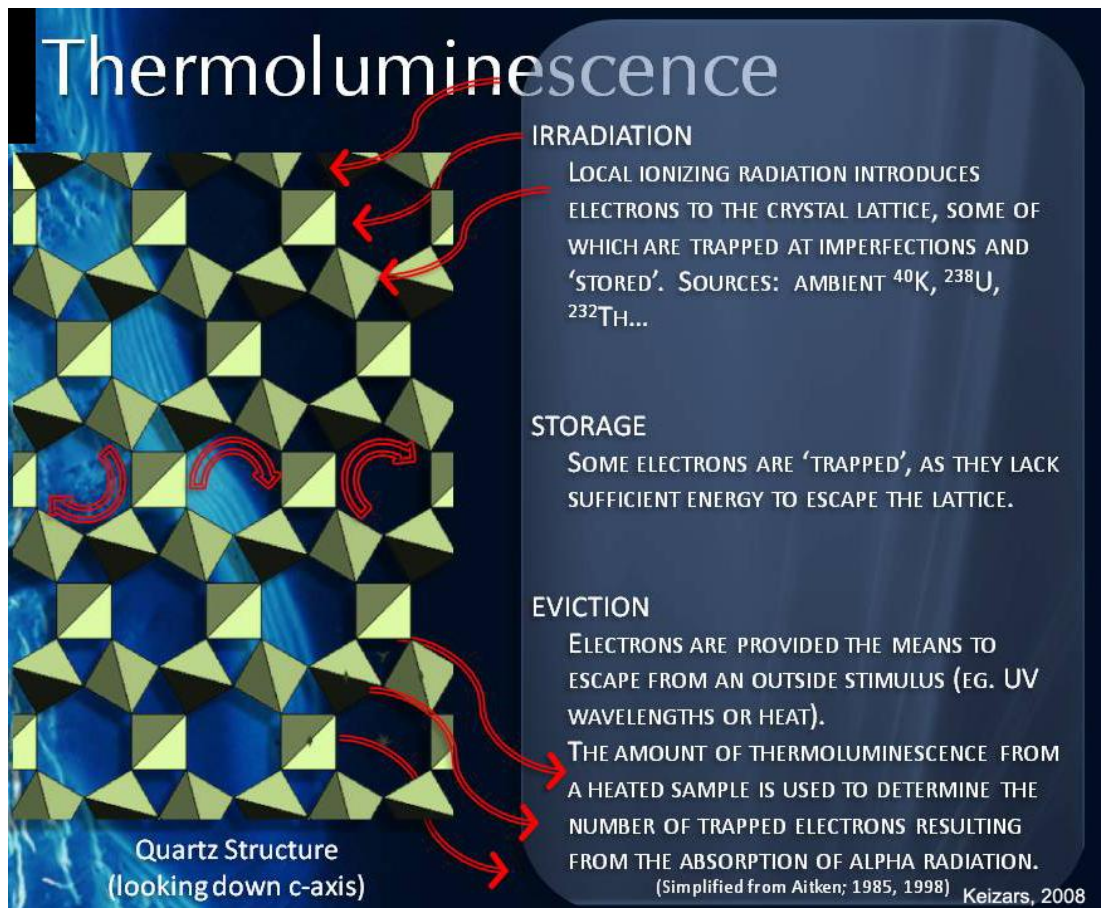


Figure 1: The three stages of thermoluminescence as outlined by (Aitken 1985, 1998) and applied to a quartz grain (Keizars, 2008b)

1.1.1.1 Trapping

Electrons of an atom forming the crystal lattice of a material become freely mobile and come to conduction band when it is exposed to radiation. Structural defects in the lattice (vacancies, interstitial atoms, and substitutional impurities) create localized charge deficits, which act as traps T for the conduction electrons. Some of these excited electrons go back to its ground state energy level after irradiation, but some are trapped at deep traps and remain there over geological time-scales. At that

time the charge deficient center which contributed the trapped charge becomes a luminescence center L. (Figure 2)

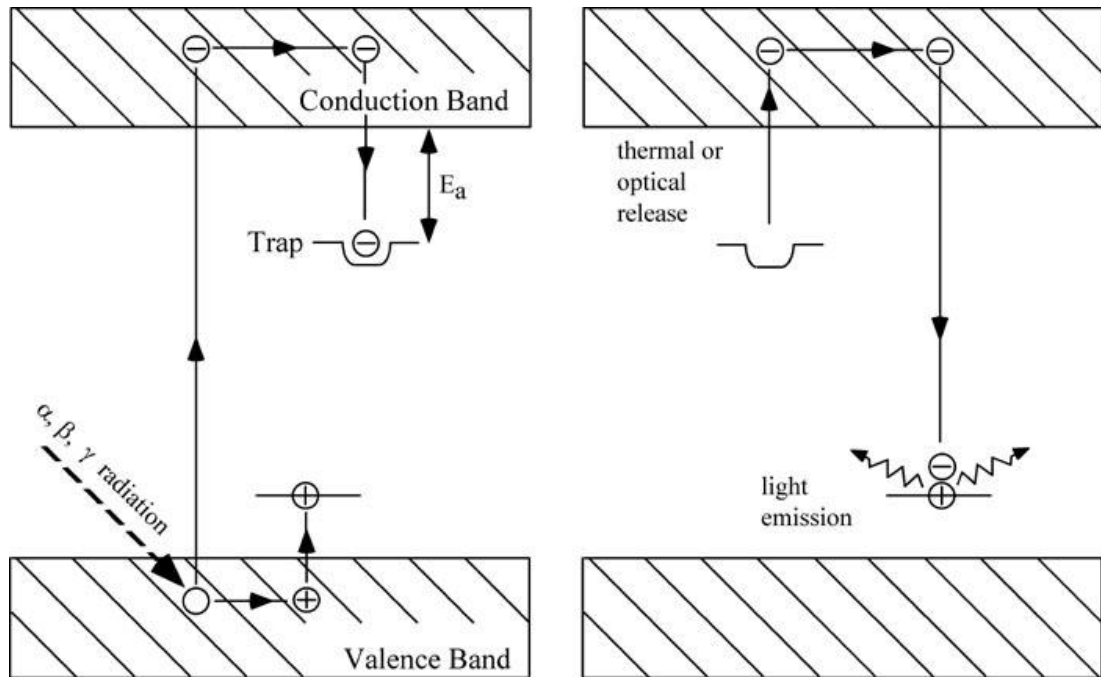


Figure 2: Trapping of excited electrons upon exposure to radiation and recombination of trapped electrons upon external activation energy. (http://rses.anu.edu.au/research/ee/resources/index.php?p=trapped_charge)

1.1.1.2 Recombination

Trapped electrons cannot escape from those traps unless activation energy is applied on them. By heating or giving light as external activation energy, these trapped electrons can go up to conduction band and then relaxes, in other words go back to its original ground state. When these electrons meet a luminescence center L, a photon is emitted. This process is called recombination. (Figure 2)

1.1.2 APPLICATIONS OF THERMOLUMINESCENCE

1.1.2.1 Radiation dosimetry

The detection of absorbed dose to people and to the environment is one of the several purposes of dosimetry applications. It is possible to measure doses as small as those caused by the natural environment over a period of several days, or doses as high as those delivered inside a nuclear reactor with a dose difference factor of approximately 10^{11} by applying radiation dosimetry method. In the following part the range of uses of TL in radiation dosimetry will be described:

1.1.2.1.1 *Dosimetry applications*

1.1.2.1.1.1 Personnel dosimetry

Personnel dosimetry is used to monitor the radiation dose absorbed by the personnel during routine occupational exposure. The dose equivalent range of interest is from approximately 10^{-5} Gy to 10^{-1} Gy, with a required uncertainty of better than $\pm 10 - 20$. (One gray (Gy) is the absorption of one joule of energy, in the form of ionizing radiation, by one kilogram of matter (human body)).

1.1.2.1.1.2 Environmental dosimetry

The measurement and controlling of radiation released to the environment is a problem for especially industrialized countries and TLD usage is an important necessity in this type of activity. Since exposure levels are low (with equivalent doses of, typically, 10^{-5} Gy) long exposure times are required and, thus, long term stability of TLD becomes vitally important, along with extreme sensitivity.

1.1.2.1.1.3 Medical dosimetry

Medical dosimetry can be used for clinical radiation exposure of humans in diagnostic radiology (e.g. x-ray exposure in mammography, dentistry and general health screening) and radiotherapy (primarily cancer therapy of various types). Doses equivalent range varies from 10^{-5} to 1 Gy in radiology and up to 10 Gy in radiotherapy.

The most important property of medical dosimeters is the tissue equivalency. Also it is necessary to be non-toxic and to have high sensitivity in order to keep the dosimetric material amount as small as possible for in vivo measurements.

1.1.2.1.1.4 Retrospective dosimetry

In the determination of previously irradiated radiation dose in accidentally contaminated areas, retrospective dosimetry is used. Chernobyl (Byelorussia and Ukraine) and Techa River (Russia) along with similar efforts at Hiroshima and Nagasaki (Japan) and the Nevada Bomb Test Site (US) are the examples of these types of areas where retrospective dosimetry is needed.

1.1.2.1.1.5 High dose

Materials testing, food sterilization and other similar applications require the use of very high doses (10^2 Gy to 10^6 Gy) of irradiation and TLDs have also found application in these high dose regimes.

1.1.2.2 TL dating of archeological and geological samples

Another important application of TL is its use in the dating of archeological and geological samples. (R. Chen, S. W. S. McKeever, 1997)

1.1.3 THERMOLUMINESCENCE DOSIMETRY

Thermoluminescence dosimetry (TLD) deals with the measurement of ionizing radiation by means of radiation-induced changes in the properties of certain materials. (C. Furetta, C. 2003)

1.1.3.1 Properties of a TLD

Thermoluminescent dosimeter (TLD) needs to have some features such as; a simple glow curve structure, a high gamma ray sensitivity, low fading of TL signal, linear dose - response relationship, simple annealing procedure for reuse, chemical stability and inertness to extreme climatic variations, insensitive to daylight, suitable effective atomic number (Z_{eff}), close to that of soft tissue which is 7.42. (A. S. Pradhan, 1981)

On the other hand the main peak of the glow curve of a TLD should have a peak temperature at the maximum in the range 180 °C - 250 °C. At higher temperatures the infrared emission from both TLD sample and TLD holder may interfere giving up to a source of errors in the reading interpretation

The above properties cannot be fulfilled by only one type of TL phosphor. As a result, there is a serious limitation in the choice and the materials which can be used for dosimetry have properties which are a compromise among the various

requirements but a material can be easily found having very good performances for one or more specific applications.

1.1.3.2 Glow Curve

Glow curve is the plot of TL intensity versus heating temperature. Glow curve may contain single or several peaks which belongs to different trapping levels. These peaks may be well resolved or overlapped.

Glow curve is characteristic for each dosimetric material but may vary in intensity with varying the dose of radiation applied and the amount of sample. There also may be shifts in glow peaks in glow curve by changing the heating rate during read out process.

1.1.3.3 Dosimetric Peak

Dosimetric peak is a well resolved, stable and high intensity peak in glow curve, which is characteristic for every dosimetric material. Dosimetric peak is important for determination of given dose of radiation. (C. Furetta, C. 2003)

1.1.3.4 Error sources in TLD measurements

There might be some errors in reading the irradiated samples caused from dosimeter, reader or annealing procedure.

Sources of error due to the dosimeter can be summarized as; variation of transparency and other optical properties of the dosimeter, effects due to the artificial light and/or natural light (optical fading), effects due to the energy dependence of the TL response, effects due to the directional dependence of the incident radiation on the thermoluminescent response, non-radioactive contaminations of the phosphor and/or the detector, non-efficient and non-reproducible procedure for cleaning the dosimeter, variations in the mass and size of the TL material, non-uniform distribution of the TL material on the reader tray when powder is used, loss of TL signal owing to thermal fading, or increase of the TL background due to environmental radiations. Background dose or in other words zero dose of the TLD sample would be an important source of error especially during low dose reading of TL because data or signal can be lost below the background. But it is reasonable to get more reliable results in higher doses since the signal is relatively higher than the background of TLD.

Errors associated with the reader can be generated by an unsuitable or instable readout cycle, as well as by non-reproducibility of the detector position in the reader tray. Also using planchet in readers as heating element, an error is generated by a poor thermal contact between detector and heater. If powder TLD samples are being used instead of film batches of chips, this can cause contamination of the photomultiplier tube. In the loss of irradiated powder in the reading chamber, this dirt produces abnormal high background signals during successive use of the reader.

Errors due to the annealing procedures can be summarized as in the following. It has well been demonstrated that the non-reproducibility of the annealing procedure can cause large variations in the sensitivity of the TL materials. It is recommended to carry out thermal erasing procedure in oven. An in-reader anneal can be done just in the case where very low irradiation doses have been detected and also in that case to be sure about the advantage of the procedure in terms of reproducibility in the measurements.

For each TL material the proper annealing procedure must be determined and checked, both in temperature and time. The best combination of temperature and time will produce an effective depletion of the traps.

Another important factor which can introduce error in the dose determination concerns the cooling rate after annealing. As the cooling rate changes, the sensitivity changes dramatically. This effect is observed in any kind of TLDs. (C. Furetta, C. 2003)

1.1.3.5 Dosimeter's Background

Although a dosimeter did not irradiated before measurement, it is possible to observe some amount of radiation absorbed by the dosimetric material. This TL signal is called dosimeters background or zero dose reading.

The reason for the background can be stimulation of the TL phosphor by UV and visible light, infrared emission of the heating element and its surroundings, dark current fluctuations of the photomultiplier tube, residual signals from the TL phosphor due to previous irradiations.

1.1.3.6 Annealing

Dosimetric materials may be affected from any radiation and stores this radiation inside their structures. Previously stored radiation can cause errors in measuring the dose of radiation applied gradually so; unconscious radiation stored has to be erased and irradiation memory has to be deleted before irradiation. This process is called annealing.

Annealing process consist of a heating treatment up to a pre-determined temperature for a pre-determined duration and a cooling process to room temperature.

Different types of dosimetric materials have different annealing process. Some of the known dosimetric materials need complex annealing procedure. LiF:Mg,Ti is one of these kind of problematic materials. It has to be annealed in two steps; firstly high temperature annealing for dosimetric traps of residual signal and then low temperature annealing for stabilization and aggregation of low temperature traps. (C. Furetta, C. 2003)

Annealing procedure for a material has to be determined once and has to be used for all samples of this material for reproducible TL applications. (G. Busuoli, C. 1981)

1.1.3.7 The Effects of Heating Rate on TL Results

Heating rate affects the TL results of a material. Gorbics et al. reported the effects of heating rate on TL results as following:

- The maximum glow-peak temperature is shifted to higher temperatures as the heating rate increases.
- The TL intensity decreases as the heating rate increases. (S.G. Gorbics, 1968)

Heating rate should be standard for all measurements in order to have reliable results in a batch of dosimeters or dosimetric materials.

1.2 LITHIUM TETRABORATE

1.2.1 Physical Properties and Uses of LTB

Lithium tetraborate ($\text{Li}_2\text{B}_4\text{O}_7$) is a congruently melting compound with low melting point and small density (melting point = $916\text{ }^\circ\text{C}$, $\rho = 2.45\text{ g/cm}^3$). (M. Ishii, 2004) LTB is one of the preferred phosphors for personnel and clinical thermoluminescent dosimetry. Its effective atomic number (7.4) for photoelectric absorption is similar to that of tissue (7.42), its photon energy response shows little variation, the detection limit is very low and the annealing procedure is simple. Furthermore, the high thermal neutron capture cross sections of ^{10}B and ^6Li have promoted the application of lithium tetraborate with different isotopic contents for B and Li for neutron and mixed-field dosimetry purposes. (A. C. Fernandes, 2008) Lithium tetraborate single crystals are used in nonlinear optics, surface-acoustic-wave devices, pressure sensors, pyroelectric sensors and many other application areas. (B. M. Hunda, 2005)

1.2.2 Crystal structure of LTB

Crystal structure of LTB is characterized by the space group $I4_1cd$ belonging to the point group C_{4v} , and can be described as a $=\text{B}-\text{O}-\text{B}\equiv$ covalent network consisting of a frame of alternating oxygen-bonded BO_4 and BO_3 oxyanions and stabilized by Li^+ ions accommodated within this network. (J. Krogh-Moe, 1962) The basic structural unit of the network is a cradle-like B_4O_7 group. (G. Corradi, 2008) LTB has a tetragonal structure with lattice parameters $a = b = 9.47\text{ \AA}$ and $c = 10.26\text{ \AA}$.

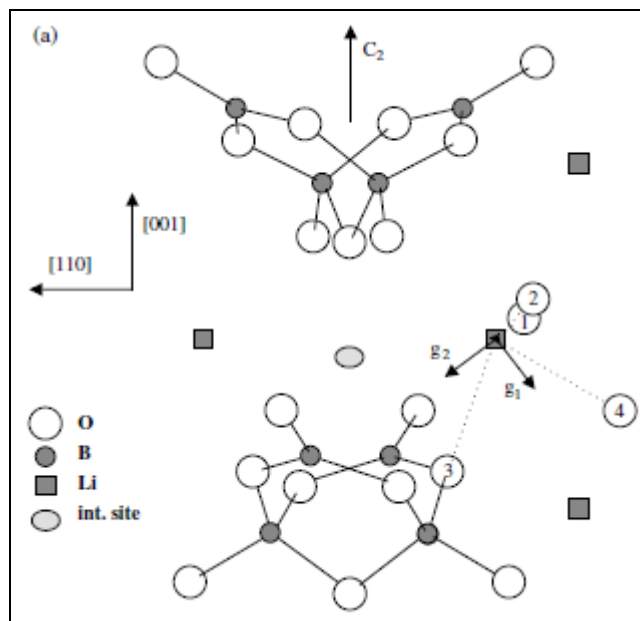


Figure 3: Structure of the $\text{Li}_2\text{B}_4\text{O}_7$ lattice shown as projections of part of the tetragonal elementary cell along a [110]-type axis. (J. Krogh-Moe, 1962)

1.2.3 FTIR Spectrum of LTB

The vibrational bands, present in FTIR spectrum of LTB, are assigned as; borate deformation, plane bending of boron oxygen triangles: 580 cm^{-1} , stretching vibrations of tetrahedral BO_4^- : $900\text{-}865\text{ cm}^{-1}$, diborate groups: 1000 cm^{-1} , pentaborate: 1080 cm^{-1} , stretching vibration of $(\text{BO}_3)^{3-}$: $1246\text{-}1807\text{ cm}^{-1}$, and stretching vibrations of B-O of trigonal $(\text{BO}_3)^{3-}$ units: $1343\text{-}1248\text{ cm}^{-1}$.

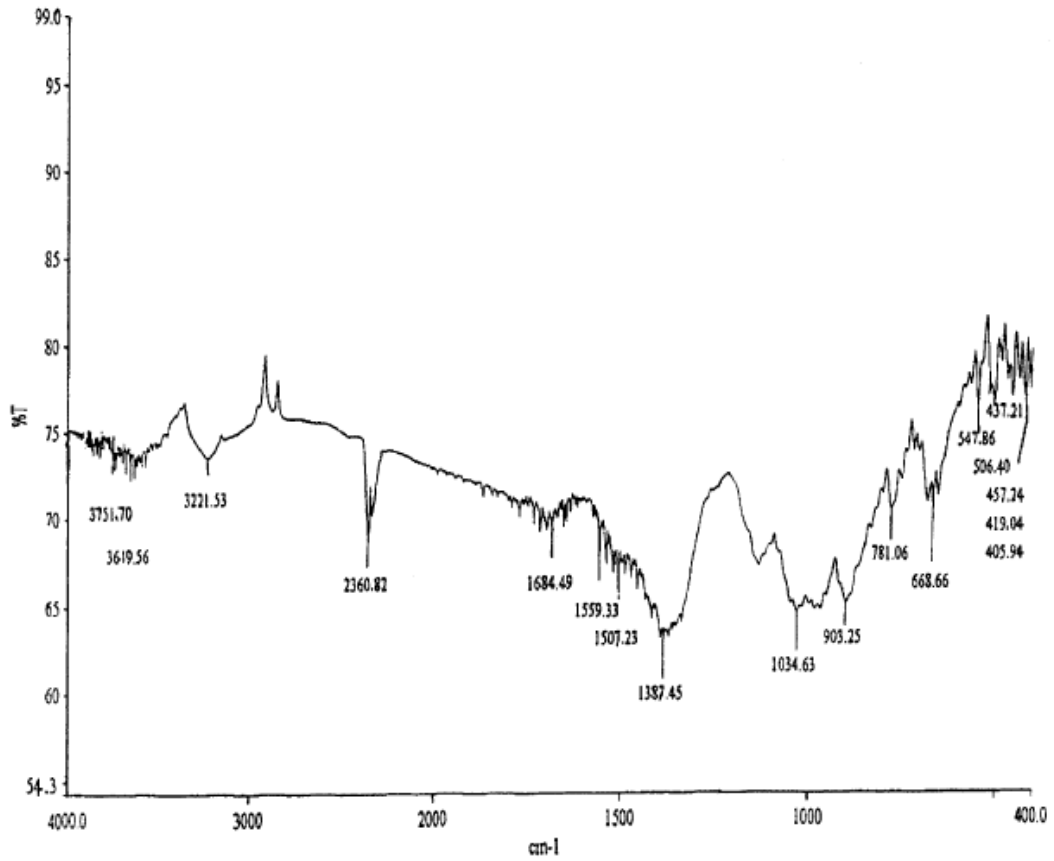


Figure 4: FTIR spectrum of $\text{Li}_2\text{B}_4\text{O}_7:\text{Cu}$ sample at room temperature (J. Manam, 2004)

1.2.4 Synthesis of LTB

1.2.4.1 Polycrystalline LTB

Sangeeta et al. produced LTB polycrystalline material by solid-state sintering method. The starting Li_2CO_3 and B_2O_3 powders taken in stoichiometric ratio were homogenized by ball milling and then sintered at 700 °C for 48 h to achieve phase formation. (Sangeeta, 2004)

Ege et al. prepared LTB samples by using wet reaction between stoichiometric amounts of Li_2CO_3 and H_3BO_3 with the addition of SiO_2 to prevent adverse effects of humidity. (A. T. Ege, 2007)

Mathews et al. prepared LTB from the starting materials Li_2CO_3 and H_3BO_3 . Appropriate quantities of these materials, to give the desired mole percent of Li_2O and B_2O_3 , were melted in platinum crucibles at $950\text{ }^\circ\text{C}$ for 15 min in a vertical furnace. The completely melted samples were quenched in Hg at room temperature. The quenched products were finely powdered and heated at $550\text{ }^\circ\text{C}$ for 48 h with intermittent grindings. (M.D. Mathews, 1998)

1.2.4.2 LTB Thin Film

Hemry et al. produced LTB thin films in order to solve the vibrational modes of bonding structures of LTB. Thin film production was carried out in two steps; solution preparation and film preparation.

1.2.4.2.1 Solution preparation

LTB has very low solubility in water, which is about 3 wt % at room temperature. On the other hand it is possible to obtain super saturated aqueous solutions of LTB up to 25 wt %. (W. T. Reburn, 1955)

The procedure requires first preparing an aqueous solution of lithium hydroxide monohydrate and then adding boric acid. For instance, an approximately 10wt% solution was obtained by adding 200 ml of water to 11 g of lithium hydroxide monohydrate stirring over low heat for 30 min giving a clear, transparent solution with pH:14, then adding 32.5 g of boric acid and continuing to stir for another 30

min giving a clear, transparent solution at pH:10. The result is a solution of the basic (i.e. hydrolyzed) salt which is reasonably stable at room temperature.

1.2.4.2.2 *Film preparation*

The thin films can be prepared from the above solution by spin-coating technique. For instance, a pipette was employed to flood the surface of the potassium bromide (KBr) disc acting as a substrate with the 10 wt% solution and the substrate was then immediately spun at 1500 r.p.m. for 30 s producing a thin gel film. (J. D. Hemry, 1998)

1.2.4.3 Single Crystalline LTB

Sugawara et al. produced single crystals of LTB by using purified $\text{Li}_2\text{B}_4\text{O}_7$ polycrystalline powder (99.99%) which was charged in a Pt crucible as a starting material. The crystals were grown in air by the Czochralski (CZ) method using a resistance heating furnace. (T. Sugawara, 1998)

The Czochralski process is a method of crystal growth used to obtain single crystals of semiconductors, metals, salts, and synthetic gemstones. The process is named after Polish scientist Jan Czochralski, who discovered the method in 1916 while investigating the crystallization rates of metals.

High-purity, polycrystalline, powder materials are melted down in a crucible, which is usually made of quartz or platinum. A seed crystal, mounted on a rod, is dipped into the molten material. The seed crystal's rod is pulled upwards and rotated at the same time. By precisely controlling the temperature gradients, rate of pulling and

speed of rotation, it is possible to extract a large, single-crystal, cylindrical ingot from the melt.

Occurrence of unwanted instabilities in the melt can be avoided by investigating and visualizing the temperature and velocity fields during the crystal growth process. This process is normally performed in an inert atmosphere, such as argon, and in an inert chamber, such as quartz. (http://en.wikipedia.org/wiki/Czochralski_process)

The Bridgman-Stockbarger technique is a method used in growing single crystal ingots.

The method involves heating polycrystalline material in a container above its melting point and slowly cooling it from one end where a seed crystal is located. Single crystal material is progressively formed along the length of the container. The process can be carried out in a horizontal or vertical geometry.

It is a popular method of producing certain semiconductor crystals, where the Czochralski process is more difficult. (http://en.wikipedia.org/wiki/Bridgman-Stockbarger_technique)

1.2.5 Doping of LTB with different metals

Doping process of LTB was done mainly in two different ways. Many scientists added Mn, Fe, Co, Mo, Cu, Ag, or Mg as dopant into LTB during or after the synthesis of LTB.

In doping process of different metals into LTB, dopant metals were added into the reactants for LTB production, and then followed by a single heat treatment process.

Dopants penetrate into the crystal structure of LTB while the crystallization is occurring.

There is another way of doping metals into LTB, which is applied in two steps; firstly the synthesis of LTB and the formation of crystal lattices, then secondly the insertion of dopant metals into the crystal structure by the help of diffusion. Second heat treatment is important for adjusting the temperature and duration, since it is necessary to prevent the deformation of structure and decomposition of host material and to assure the diffusion of dopant metal atoms into LTB.

1.2.6 TL Studies on LTB in Literature

Many researchers investigated the TL properties of LTB doped materials with different activators such as: Mn, Cu, Ag, and Mg. The first thermoluminescent material based on LTB activated by Mn is commercialized by Harshaw under the name TLD-800. (G. Kitis, 2000)

Kelemen et. al. reported the radioluminescence and thermoluminescence data for Mn doped single crystal and glassy samples of LTB, and single crystal form of the LTB:Mn was reported with a glow curve containing one peak at about 80 °C, and another peak at about 220 °C although glassy form had a very broad peak at about 150 °C. (A. Kelemen, 2008)

Wall et. al. investigated the suitability of three different thermoluminescent lithium borates; LTB:Mn, LTB:Cu and LTB:Cu,Ag. The properties of copper doped LTB powder make it more attractive for low dose measurements than manganese doped. However, the energy response of the copper doped material was not quite as suitable as that of the manganese doped material for measuring doses to tissue at photon energies lower than 100 keV. (B. F. Wall, 1982)

Driscoll et al. compared the thermoluminescence properties of Mn doped LTB powder with Cu doped LTB and Cu and Ag doped LTB on their dose-response behaviors and degrees of fading and the results of this study fitted suitable well with the results of Wall. Driscoll et al. also compared the usable dose ranges and photon energy responses for TLD-800 chips and two different Mn doped LTB obtained from two producers. According to comparison results of two different Mn doped LTB obtained from two producers, both LTB:Mn had similar properties which were investigated. (C. M. H. Driscoll, 1983)

Lorrain et. al. doped transition elements including Mn and rare earths into LTB and compared the thermoluminescence results of doped LTB. Lorrain reported a LTB:Mn glow curve with one peak at about 100 °C and another peak at 235 °C which is produced by using a completely new doping method which is called Lorrain doping. (S. Lorrain, 1986)

Kitis et. al. reported a study on the kinetic parameters of LTB:Mn,Si, LTB:Cu, LTB:Cu,In and MgB₄O₇:Dy,Na. Kitis et. al. also implied that LTB:Mn has a very poor sensitivity, mainly caused by the light emission in the 600nm region of the spectra, far from the response region of most of the photomultipliers used in commercial readers. (G. Kitis, 2000)

Park et. al. compared the thermoluminescence and photoluminescence results of Cu, Mn and Mg doped LTB single crystals. LTB:Cu had a glow curve consisting of three peaks, one is at 125 °C, one is at 210 °C, and the other one is at about 260 °C. LTB:Mg gave a glow curve with only one peak at about 200 °C, although LTB:Mn gave a peak at about 250 °C. (Kang-Soo Park, 2003)

Holovey et. al. focused on the thermoluminescent behaviors with different annealing conditions of LTB:Mn single crystals. (V. M. Holovey, 2007)

In the research area of thermoluminescence properties of materials, our group was focused on lithium borates. Zeynep Özdemir was the first member worked with lithium triborate which is one of the lithium borates. Özdemir tried to synthesize lithium triborate (LiB_3O_5) and doped lithium triborate with CuO , MnO_2 , Fe_2O_3 , CoCO_3 , MgO , and Al_2O_3 with varying concentrations from 0.1 wt % to 1 wt % in lithium triborate. 0.4 wt % and 0.7 wt % CuO doped and 1 wt % Al_2O_3 doped lithium triborate gave promising TL response. (Z. Özdemir, 2006) Burcu Ardıçoğlu, doped lithium triborate with 3 different rare earth metals Gd_2O_3 , La_2O_3 , and Y_2O_3 , but the TL response results of rare earth metal doped lithium triborate were not as good as CuO doped or Al_2O_3 doped lithium triborate and not applicable to produce a dosimetric material. (B. Ardıçoğlu, 2005) Tolga Depçi, one of the other members of our group, took the results of Özdemir's results on Al_2O_3 doped lithium triborate one step further. 5 wt % Al_2O_3 doped lithium triborate gave a very stable high intensity TL glow peak at 200 °C. (T. Depçi, 2009) Esin Pekpak worked on another lithium borate which is lithium tetraborate ($\text{Li}_2\text{B}_4\text{O}_7$). Pekpak doped lithium tetraborate with Cu , Ag and In with different combinations and concluded that 0.1 wt % Cu doped and 0.1 wt % Cu , 0.4 wt % Ag gave promising TL response results. (E. Pekpak, 2009)

OBJECTIVE

In this study it was aimed to investigate the effects of Mn doping into LTB on TL glow curves and to investigate if there is any effect of synthesis and doping methods on glow curves. Additionally the effects of addition of Ag , Mg and P as co-dopants were also investigated. In order to understand those, LTB was synthesized with two different methods; one was solid synthesis and to other one was wet synthesis methods. Dopant amount and doping methods were also varied.

CHAPTER 2

MATERIALS, EQUIPMENTS, AND METHODS

2.1 MATERIALS

All of the chemicals used in experimental studies are listed below.

In the production of LTB, Li_2CO_3 , H_3BO_3 , $(\text{NH}_2)_2\text{CO}$, and distilled water was used. $\text{MnCl}_2 \cdot 4\text{H}_2\text{O}$, AgNO_3 , MgCl_2 , $\text{NH}_4\text{H}_2\text{PO}_4$, were used in doping procedures as dopant sources.

2.2 EQUIPMENTS

2.2.1 Furnace

Solid-state reactions have been carried out in air by using Protherm furnace with heating ability up to 1300 °C and the heating procedure control option.

2.2.2 Powder X-Ray Diffractometer

The powder XRD patterns were recorded using a Rigaku diffractometer, equipped with a Miniflex goniometer and an X-ray source with $\text{CuK}\alpha$ radiation, at $\lambda = 1.5418$ Å, 30 kV and 15 mA. The powder samples were pressed and affixed to standard-sized glass slides and scanned in the 5–70°, 2θ range with a scan rate of 2 degree per min.

Diffraction patterns were assigned using Joint Committee on Powder Diffraction Standards (JCPDS) cards supplied by the International Centre for Diffraction Database (ICDD) card numbered 18-0717.

2.2.3 Fourier Transform Infrared Spectrometer

Fourier transform infrared (FTIR) spectroscopic measurements were carried out in transmission mode, using (VARIAN 1000) FTIR spectrometer, equipped with KBr windows working in the range of 400-4000 cm^{-1} . Each spectrum was acquired with a resolution of 4 cm^{-1} and by averaging over 128 scans. Pellets for FTIR analysis were prepared such that powder samples were supported with dehydrated-KBr in the ratio of 3 mg: 100 mg.

2.2.4 Scanning Electron Microscope

Morphologies of the synthesized samples were investigated using a scanning electron (SE) microscope. SEM data were acquired using a Zeiss SUPRA 50 VP which has magnification range between 12-900000 and variable pressure between 2-133Pa. SEM that is equipped with a FE electron gun, a vacuum SE detector and an elevated pressure SE detector. Samples for SEM analysis were prepared by grinding the powder samples into fine particles and mechanically dispersing them on an electrically conductive carbon film which was placed on an aluminum sample holder. No additional coatings or dispersive liquids were used for the SEM preparation. All of the SEM images were obtained using a vacuum SE detector where electron acceleration voltage of the incident beam was varied within 0.1-30 kV and the samples were kept typically at $\leq 5 \times 10^{-5}$ Torr inside the SEM.

2.2.5 Inductively Coupled Plasma Optical Emission Spectrometer

The actual amount of dopants in LTB was determined by using Perkin Elmer Optima 4300DV Inductively Coupled Plasma Optical Emission Spectrometer. Sample solution was prepared by using microwave oven.

2.2.6 Thermoluminescence Reader

The dosimetric properties of the samples were determined by using Harshaw TLD Reader Model 3500. The heating rate was chosen as the lowest possible for the measurements to be most reliable. As a result, the heating rate of 1 °C/sec was adapted from 50 °C to 400 °C. The examined dosimeters were exposed to Beta, ⁹⁰Sr-⁹⁰Y radiations at room temperature for 5 minutes while the radiation given was 0.9 Gy/min. The sample amount was 20 mg which is within the reliable range determined by (B. F. Wall, 1982).

2.3 EXPERIMENTAL METHODS

2.3.1 Synthesis of LTB

Synthesis of LTB was carried out with 2 different techniques. The first method was wet synthesis, and the second method was high temperature solid state synthesis method.

2.3.1.1 Wet synthesis

In the production of LTB with wet synthesis method, 3.7098 g of H_3BO_3 and 0.7388 g of Li_2CO_3 in powder form were dissolved in about 15 ml of distilled water by heating gently and stirring in a beaker on a magnetic heating stirrer. After dissolution of reactants in water, a clear solution was formed. Continuing heating and stirring resulted with a viscous transparent liquid, which contains dissolved H_3BO_3 and Li_2CO_3 . After taking this viscous liquid into a platinum crucible, it was put into a furnace and heated up to 150 °C for 2 hours to remove extra water from the reaction medium. After this 2 hours treatment, it was continued heating up to 750 °C with a heating rate of 350 °C / hour. The reactants kept at this temperature for 1 hour to complete the reaction. At the end of the reaction, the product was cooled down to room temperature and grinded in an agate mortar.

2.3.1.2 High temperature solid state synthesis (solid synthesis)

In the production of LTB with high temperature solid state synthesis method, 3.7098 g of H_3BO_3 and 0.7388 g of Li_2CO_3 in powder form were weighed and mixed in an agate mortar. The mixture of reactants was put into a platinum crucible and put into the furnace. The reactants were firstly heated up to 400 °C with a heating rate of 350 °C / min and it is kept at that temperature for 3 hours to let the evaporation of water liberated during the conversion of H_3BO_3 to B_2O_3 and the removal of CO_2 . After 3 hours the intermediate was grinded and pounded in an agate mortar and again put into the crucible. The intermediate was put into a furnace to heat up to 750 °C and kept at that temperature for 2 hours. After cooling the product, it was grinded and pounded again and put into the furnace once more to repeat the 750 °C heat treatment for 2 hours. Finally the product was cooled down to room temperature and grinded lastly.

2.3.2 Doping of metals into LTB

LTB powders synthesized in wet and solid synthesis methods were doped with Mn with a varying content from 0.1 wt % to 10 wt % by applying two different doping methods. The following experimental chart (Table 2) shows the matrix of different synthesis and doping methods for LTB doped with Mn in different amounts.

Table 2: Experiment chart for different synthesis and doping methods

	Wet synthesis	Solid synthesis
Wet doping	0.1 wt % Mn	0.1 wt % Mn
	0.5 wt % Mn	0.5 wt % Mn
	1 wt % Mn	1 wt % Mn
	2 wt % Mn	2 wt % Mn
	3 wt % Mn	3 wt % Mn
	4 wt % Mn	4 wt % Mn
	5 wt % Mn	5 wt % Mn
	6 wt % Mn	6 wt % Mn
	7 wt % Mn	7 wt % Mn
	8 wt % Mn	8 wt % Mn
9 wt % Mn	9 wt % Mn	
10 wt % Mn	10 wt % Mn	
Solid doping	0.1 wt % Mn	0.1 wt % Mn
	0.5 wt % Mn	0.2 wt % Mn
	1 wt % Mn	0.3 wt % Mn
	2 wt % Mn	0.4 wt % Mn
	3 wt % Mn	0.5 wt % Mn
	4 wt % Mn	0.6 wt % Mn
	5 wt % Mn	0.7 wt % Mn
	6 wt % Mn	0.8 wt % Mn
	7 wt % Mn	0.9 wt % Mn
	8 wt % Mn	1 wt % Mn
9 wt % Mn	2 wt % Mn	
10 wt % Mn	3 wt % Mn	
	4 wt % Mn	
	5 wt % Mn	
	6 wt % Mn	
	7 wt % Mn	
	8 wt % Mn	
	9 wt % Mn	
	10 wt % Mn	

According to earlier results of TLD measurements solid doping of Mn into solid doped LTB powder was chosen to investigate in more detail. Ag, Mg or P was doped with Mn into solid synthesized LTB by applying solid doping. Table 3 indicates the co-doping studies of LTB done in this research.

Table 3: Experiment chart for co-doping studies

Ag co-doped	Mg co-doped	P co-doped
0.1 wt % Mn + 0.5 wt % Ag	0.1 wt % Mn + 0.5 wt % Mg	0.1 wt % Mn + 0.5 wt % P
0.2 wt % Mn + 0.5 wt % Ag	0.2 wt % Mn + 0.5 wt % Mg	0.2 wt % Mn + 0.5 wt % P
0.3 wt % Mn + 0.5 wt % Ag	0.3 wt % Mn + 0.5 wt % Mg	0.3 wt % Mn + 0.5 wt % P
0.4 wt % Mn + 0.5 wt % Ag	0.4 wt % Mn + 0.5 wt % Mg	0.4 wt % Mn + 0.5 wt % P
0.5 wt % Mn + 0.5 wt % Ag	0.5 wt % Mn + 0.5 wt % Mg	0.5 wt % Mn + 0.5 wt % P
0.6 wt % Mn + 0.5 wt % Ag	0.6 wt % Mn + 0.5 wt % Mg	0.6 wt % Mn + 0.5 wt % P
0.7 wt % Mn + 0.5 wt % Ag	0.7 wt % Mn + 0.5 wt % Mg	0.7 wt % Mn + 0.5 wt % P
0.8 wt % Mn + 0.5 wt % Ag	0.8 wt % Mn + 0.5 wt % Mg	0.8 wt % Mn + 0.5 wt % P
0.9 wt % Mn + 0.5 wt % Ag	0.9 wt % Mn + 0.5 wt % Mg	0.9 wt % Mn + 0.5 wt % P
1.0 wt % Mn + 0.5 wt % Ag	1.0 wt % Mn + 0.5 wt % Mg	1.0 wt % Mn + 0.5 wt % P

2.3.2.1 Wet doping method

In order to dope LTB with Mn, proper amount of $MnCl_2 \cdot 4H_2O$ was dissolved in distilled water. Previously synthesized LTB powder was added into the solution and stirred with a magnetic stirrer for 10 min. The suspension of LTB in Mn solution was put into a crucible and put into the furnace. Heat treatment was applied up to 150 °C for 2-3 hours to evaporate water from the medium. After all of the water removed it was continued heating up to 750 °C and kept at this temperature for 6 hours. After all of these processes the product was cooled down to room temperature and grinded to get fine powders of Mn doped LTB.

2.3.2.2 Solid doping method

In solid doping of Mn into LTB, proper amount of $\text{MnCl}_2 \cdot 4\text{H}_2\text{O}$ was weighed and mixed with LTB in powder form in an agate mortar to get a homogeneous powder mixture. The mixture of LTB and $\text{MnCl}_2 \cdot 4\text{H}_2\text{O}$ was put into a crucible and then put into the furnace to heat up to $750\text{ }^\circ\text{C}$ with a heating rate of $350\text{ }^\circ\text{C} / \text{min}$. the temperature was kept constant for 6 hours as in wet doping process. After 6 hours heat treatment the product was cooled down to room temperature and grinded to get fine powders of Mn doped LTB.

As in the wet doping process Ag, Mg or P was added as co-dopant with Mn. AgNO_3 , MgCl_2 , or $\text{NH}_4\text{H}_2\text{PO}_4$ powders were weighed and mixed with $\text{MnCl}_2 \cdot 4\text{H}_2\text{O}$ and LTB powders in an agate mortar. The mixture was then put into a furnace to heat up to $750\text{ }^\circ\text{C}$ for 6 hours. Finally the product was cooled down and grinded to get fine powders.

CHAPTER III

RESULTS AND DISCUSSIONS

3.1 Characterization

3.1.1 Powder X-Ray Diffraction (XRD)

XRD results revealed that LTB was successfully synthesized via wet and solid routes. Most intense peaks of the both two x-ray diffraction patterns of LTB samples were assigned by the help of corresponding reference data (ICDD card no 18-0717). Diffraction patterns were fitted with the reference data of LTB with tetragonal structure and cell parameters $a = 9.477$, $b = 9.477$, and $c = 10.286$. There are only a few number of peaks which are not belong to LTB were assigned as lithium triborate (LiB_3O_5) (ICDD card no 70-0735) and lithium octaborate ($\text{Li}_2\text{B}_8\text{O}_{13}$) (ICDD card no 47-0339) peaks. (Figure 5)

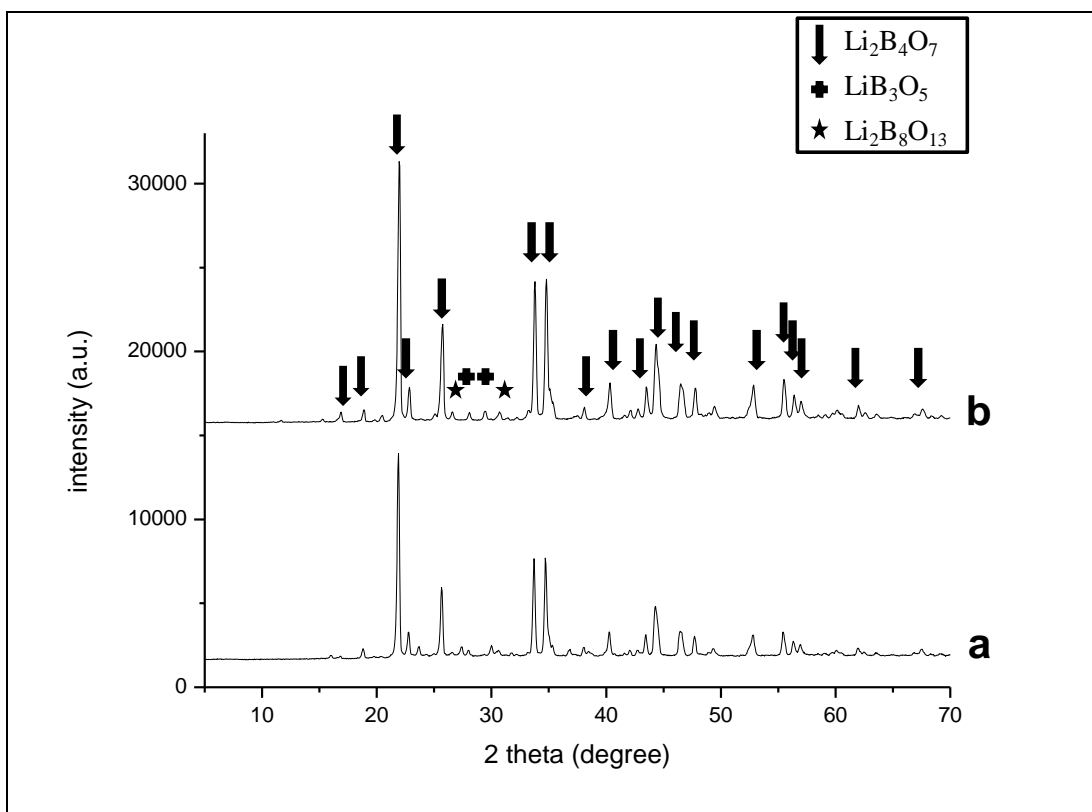


Figure 5: XRD patterns of Wet synthesized undoped LTB (a), solid synthesized undoped LTB (b).

In XRD patterns of undoped and doped products, peaks which were present in undoped LTB and not belong to LTB were disappeared by extra heating process while doping. Extra heating did not make any change in intensities of peaks in the patterns.

In comparison of wet and solid synthesized Mn doped LTBs, peak intensities and peak positions were similar with each other. Also there were no other structures belonging to impurities in XRD patterns. There were no differences in full width at half maximum values of wet and solid synthesized and doped products.

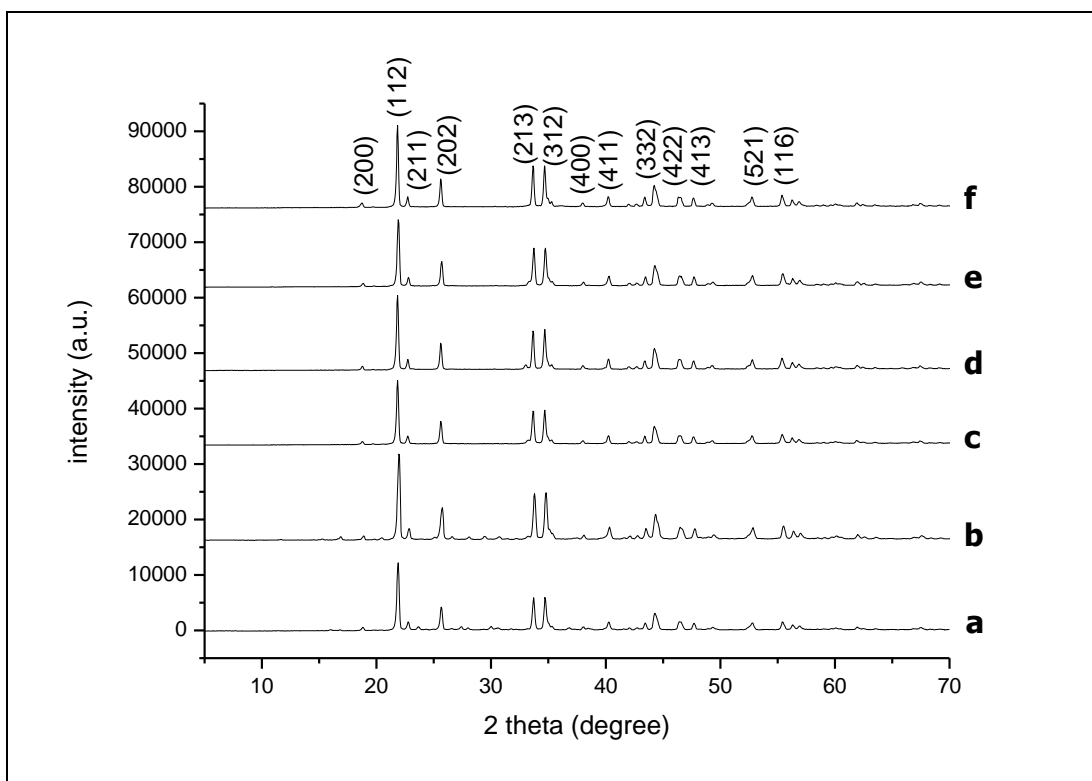


Figure 6: XRD patterns of wet synthesized undoped LTB (a), solid synthesized undoped LTB (b), wet synthesized 1 wt % Mn wet doped LTB (c), wet synthesized 1 wt % Mn solid doped LTB (d), solid synthesized 1 wt % Mn wet doped LTB (e), and solid synthesized 1 wt % Mn solid doped LTB (f). Planes of LTB are shown on the top pattern.

In order to see if there were any structural differences between differently synthesized and differently doped samples, XRD patterns of wet synthesized-wet doped, wet synthesized-solid doped, solid synthesized-wet doped, and solid synthesized-solid doped LTB:Mn samples were compared with undoped samples. There were no difference between 4 doped samples neither in peak positions and cell parameters, nor in peak intensities and peak widths. It was obvious to see that there were no structural differences between these 4 different samples.

In further investigation of XRD patterns and crystal data of differently synthesized undoped, doped and co-doped LTB samples, comparison of observed and calculated d-spacing values for LTB revealed that, the synthesized products by using wet and solid methods were obviously LTB containing a small amount of lithium triborate and lithium octaborate. Comparison of observed and calculated d-spacing values of solid synthesized and 1 wt % Mn solid doped LTB can be seen in Table 4. As it can be seen, only a few number of d-spacing values were present which are not belongs to LTB, but none of these values are indicating the presence of Mn.

In Table 5 and 6, observed d-spacing values of differently synthesized undoped, doped and co-doped LTB samples were listed and compared with calculated d-spacing values of LTB. Also Table 5 and 6 were not showing any evidence of Mn presence. Although the amount of Mn present in the LTB was up to 10 wt %, it was not possible to observe any Mn related peaks in XRD patterns. Very well mono-dispersion of Mn can prevent the detection of Mn signals in XRD.

Table 4: X-ray analysis results for solid synthesized and 1 wt % Mn solid doped LTB.

hkl	Pos. [°2Th.]	d calculated [Å]	d observed [Å]	Rel. Int. [%]
200	18.704	4.740	4.728	8
112	21.764	4.080	4.064	100
211	22.676	3.918	3.914	18
202	25.538	3.485	3.477	40
213	33.599	2.665	2.661	40
312	34.616	2.589	2.587	55
004	34.866	2.571	2.565	6
321	35.205	2.547	2.544	8
400	37.948	2.369	2.369	6
411	40.169	2.243	2.241	14
402	41.945	2.152	2.149	4
420	42.630	2.119	2.118	4
323	43.338	2.086	2.083	10
332	44.162	2.049	2.047	25
224	44.367	2.040	2.036	12
422	46.306	1.959	1.957	10
314	46.507	1.951	1.949	8
413	47.592	1.909	1.907	10
215	49.181	1.851	1.849	4
521	52.745	1.734	1.734	8
116	55.292	1.660	1.658	8
424	56.212	1.635	1.634	6
325	56.779	1.620	1.618	4
600	58.393	1.579	1.579	2
523	58.926	1.566	1.564	2
532	59.595	1.550	1.549	2
611	60.021	1.540	1.539	2
415	60.324	1.533	1.531	2
620	61.886	1.498	1.498	4
316	62.348	1.488	1.487	2
541	63.440	1.465	1.465	2
631	66.759	1.400		2
406	67.357	1.389	1.387	4
534	68.193	1.374	1.373	6
543	69.052	1.359	1.358	2

Table 5: Observed d-spacing values for different samples, and theoretical d-spacing values for $\text{Li}_2\text{B}_4\text{O}_7$.

Wet Synthesis Undoped	Solid Synthesis Undoped	Wet Synthesis Wet Doped	Wet Synthesis Wet Doped	Wet Synthesis Wet Doped	Wet Synthesis Wet Doped	d calc.	Rel. Intensity (%)
5.257*	5.257*						2
4.716	4.704	4.728	4.716	4.704	4.728	4.740	8
4.055	4.046	4.064	4.064	4.055	4.064	4.080	100
3.905	3.888	3.914	3.905	3.897	3.914	3.918	18
3.470	3.457	3.477	3.477	3.463	3.477	3.485	40
3.190**	3.178**						2
2.976**	3.025**						2
2.919*	2.910*						2
2.657	2.650	2.661	2.661	2.657	2.661	2.665	40
2.583	2.579	2.587	2.587	2.583	2.587	2.589	55
2.561	2.554	2.565	2.567	2.561	2.565	2.571	6
2.540	2.537	2.540	2.540	2.540	2.544	2.547	8
2.366	2.360	2.366	2.366	2.363	2.369	2.369	6
2.239	2.236	2.241	2.241	2.239	2.241	2.243	14
2.147	2.147	2.149	2.149	2.149	2.149	2.152	4
2.116	2.113		2.116	2.116	2.118	2.119	4
2.083	2.079	2.083	2.083	2.081	2.083	2.086	10
2.045	2.043	2.047	2.047	2.045	2.047	2.049	25
2.036	2.032	2.036	2.036	2.034	2.036	2.040	12
1.955	1.953	1.957	1.957	1.955	1.957	1.959	10
1.947	1.943	1.947	1.949	1.947	1.949	1.951	8
1.905	1.903	1.907	1.907	1.905	1.907	1.909	10
1.847	1.843	1.847	1.849	1.847	1.849	1.851	4
1.732	1.731	1.734	1.732	1.732	1.734	1.734	8
1.657	1.654	1.658	1.658	1.656	1.658	1.660	8
1.633	1.630	1.634	1.634	1.633	1.634	1.635	6
1.617	1.614	1.618	1.618	1.617	1.618	1.620	4
	1.576	1.578			1.579	1.579	2
	1.564	1.563	1.564		1.564	1.566	2
1.550					1.549	1.550	2
	1.537	1.539	1.539	1.539	1.539	1.540	2
1.529	1.529	1.530		1.531	1.531	1.533	2
1.497	1.495	1.498	1.497	1.498	1.498	1.498	4
1.486	1.484	1.487	1.487	1.484	1.487	1.488	2
1.464	1.463		1.464	1.463	1.465	1.465	2
	1.397	1.399	1.402	1.397		1.400	2
1.386	1.385	1.387	1.387	1.386	1.387	1.389	4
1.373	1.371	1.374	1.373	1.374	1.373	1.374	6
	1.356	1.357	1.358		1.358	1.359	2

* assigned as LiB_3O_5 from ICDD card no 70-0735

** assigned as $\text{Li}_2\text{B}_8\text{O}_{13}$ from ICDD card no 47-0339

Table 6: Observed d-spacing values for different samples containing different co-dopants, and theoretical d-spacing values for $\text{Li}_2\text{B}_4\text{O}_7$

Ag co-doped	Mg co-doped	P co-doped	d calc.	Rel. Intensity (%)
4.728	4.716	4.728	4.740	8
4.064	4.064	4.064	4.080	100
3.905	3.905	3.914	3.918	18
3.470	3.477	3.477	3.485	40
2.657	2.657	2.661	2.665	40
2.583	2.583	2.587	2.589	55
2.561	2.565	2.565	2.571	6
2.540	2.540	2.544	2.547	8
2.366	2.366	2.369	2.369	6
2.239	2.241	2.241	2.243	14
2.149	2.149	2.152	2.152	4
2.118	2.116	2.118	2.119	4
2.083	2.083	2.085	2.086	10
2.047	2.047	2.047	2.049	25
2.036	2.036	2.036	2.040	12
1.957	1.957	1.957	1.959	10
1.947	1.947	1.947	1.951	8
1.907	1.907	1.907	1.909	10
1.847	1.847	1.849	1.851	4
1.734	1.734	1.734	1.734	8
1.657	1.657	1.658	1.660	8
1.633	1.633	1.634	1.635	6
1.617	1.618	1.618	1.620	4
1.578	1.578	1.579	1.579	2
1.564		1.565	1.566	2
1.549		1.549	1.550	2
1.539	1.540	1.540	1.540	2
1.531		1.531	1.533	2
1.498	1.498	1.499	1.498	4
1.486	1.486		1.488	2
1.464	1.464	1.465	1.465	2
1.398		1.398	1.400	2
1.386	1.386	1.387	1.389	4
1.373	1.373	1.372	1.374	6
1.358	1.359	1.358	1.359	2

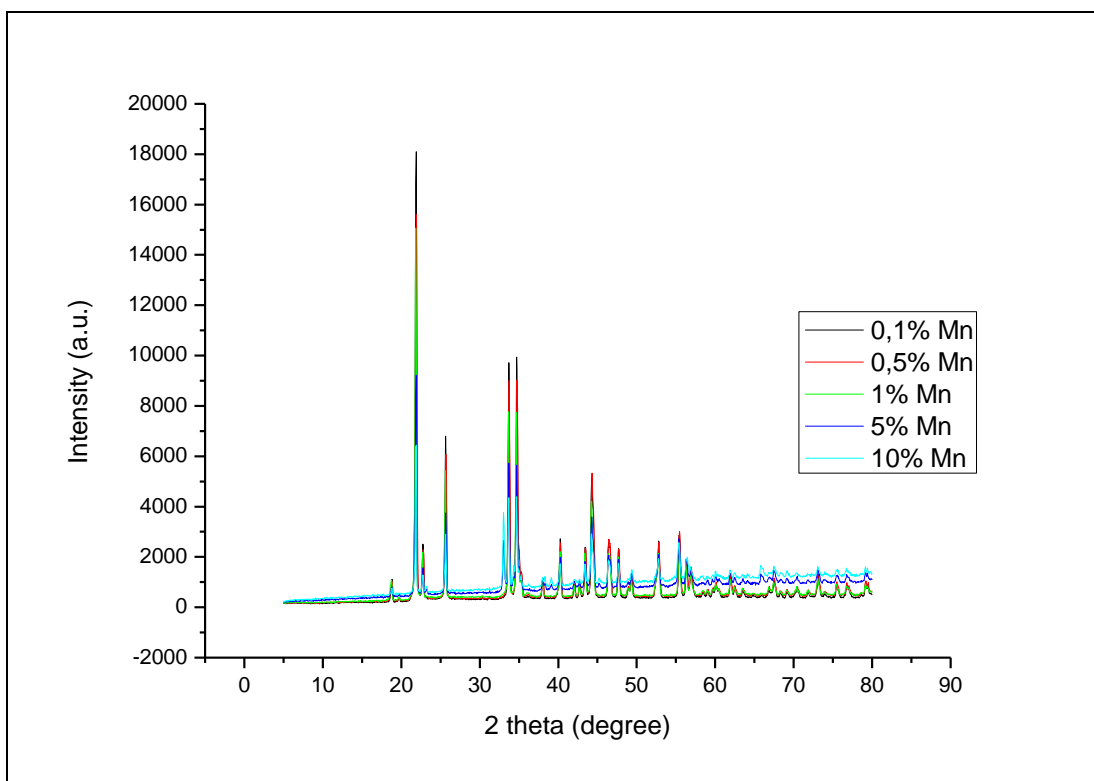


Figure 7: Comparison of XRD patterns in varying Mn content

For all of the synthesis and doping methods, in the variation of manganese content doped into lithium tetraborate, an increase is observed in the background with the increasing manganese percentage in LTB. In X-ray Diffractometer, some of the elements are problematic under Cu radiation resulting from source of diffractometer. These problematic elements are given in Figure 8. Manganese is one of these elements, which gives fluorescence under Cu radiation. This fluorescence affects the amount of diffracted beam and increases the background.

Problematic elements under Cu Radiation

H																	He
Li	Be											B	C	N	O	F	Ne
Na	Mg											Al	Si	P	S	Cl	Ar
K	Ca	Sc	Ti	V	Cr	Mn	Fe	Co	Ni	Cu	Zn	Ga	Ge	As	Se	Br	Kr
Rb	Sr	Y	Zr	Nb	Mo	Tc	Ru	Rh	Pd	Ag	Cd	In	Sn	Sb	Te	I	Xe
Cs	Ba	L	Hf	Ta	W	Re	Os	Ir	Pt	Au	Hg	Tl	Pb	Bi	Po	At	Rn
Fr	Ra	A															
		L	La	Ce	Pr	Nd	Pm	Sm	Eu	Gd	Tb	Dy	Ho	Er	Tm	Yb	Lu
		A	Ac	Th	Pa	U	Np	Pu	Am	Cm	Bk	Cf	Es	Fm	Md	No	Lr

Figure 8: Problematic elements under Cu radiation in XRD are signed with different colors (non-gray).

3.1.2 Inductively Coupled Plasma Optical Emission Spectrometer

In order to get the actual amount of dopant and to see if there was any loss of dopant during reaction, Inductively Coupled Plasma Optical Emission Spectrometry (ICP-OES) technique was applied. ICP-OES gave a result of 0.975 ± 0.003 wt % for the sample which was doped by the addition of 1 wt % of Mn and the technique assured that there was no dopant loss during doping reactions.

3.1.3 Fourier Transform Infrared Spectroscopy (FTIR)

In order to see if any differences present in bonding of atoms in LTB, FTIR spectra of differently synthesized and differently doped and undoped LTB samples were compared.

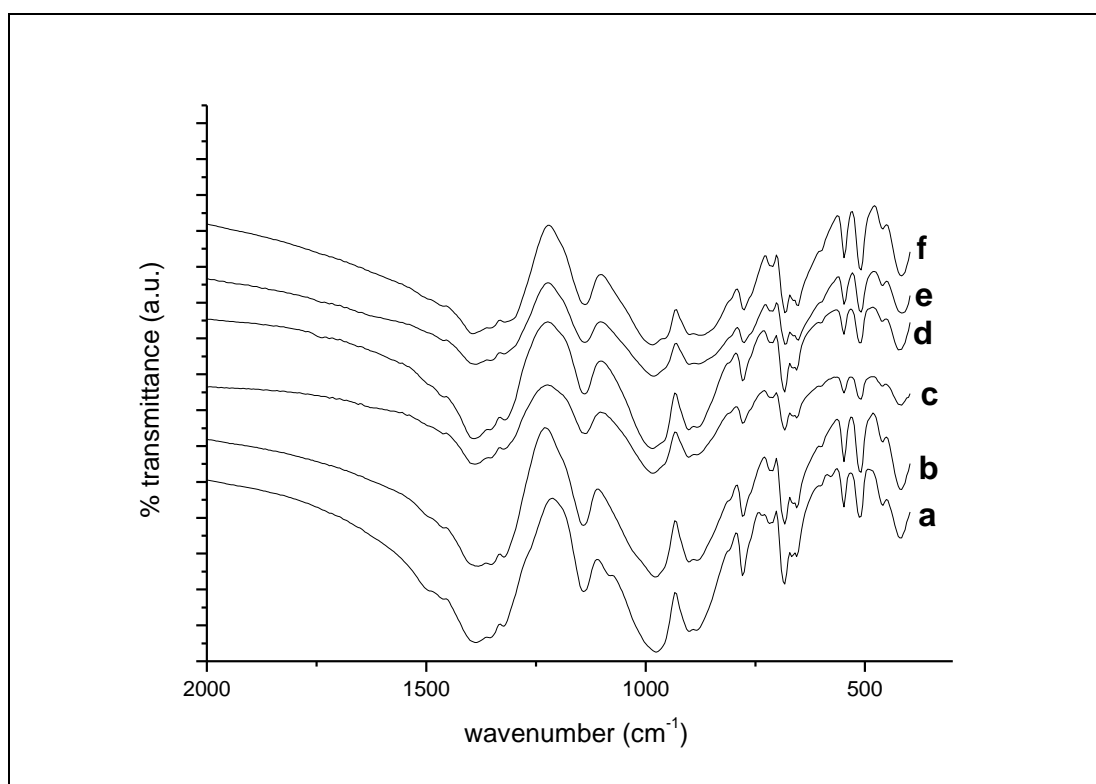


Figure 9: FTIR spectra of wet synthesized undoped LTB (a), solid synthesized undoped LTB (b), wet synthesized 1 wt % Mn wet doped LTB (c), wet synthesized 1 wt % Mn solid doped LTB (d), solid synthesized 1 wt % Mn wet doped LTB (e), and solid synthesized 1 wt % Mn solid doped LTB (f).

Also FTIR spectrums of all doped and undoped samples well agreed with the XRD results about the Mn content. (Figure 9) There were no Mn-O, Mn-B or Mn-Li vibrations seen on the spectrums. All of the other bands were well fitted with the literature values for BO_3 and BO_4 ring structure vibrations. Asymmetric B-O

stretching modes of planar BO_3^{3-} groups show bands in $1500\text{-}1200\text{ cm}^{-1}$ region. Bands in the $1100\text{-}940\text{ cm}^{-1}$ region are due to asymmetric and symmetric BO_4 stretching vibrations.

There was a very weak band at 1080 cm^{-1} in Figure 9 (a) which was not observed in solid synthesized undoped or wet and solid synthesized and doped products. This band was resulted from uncoordinated CO_3^{2-} vibrations. (A. Davydov, C. 2003)

3.1.4 Scanning Electron Microscopy (SEM)

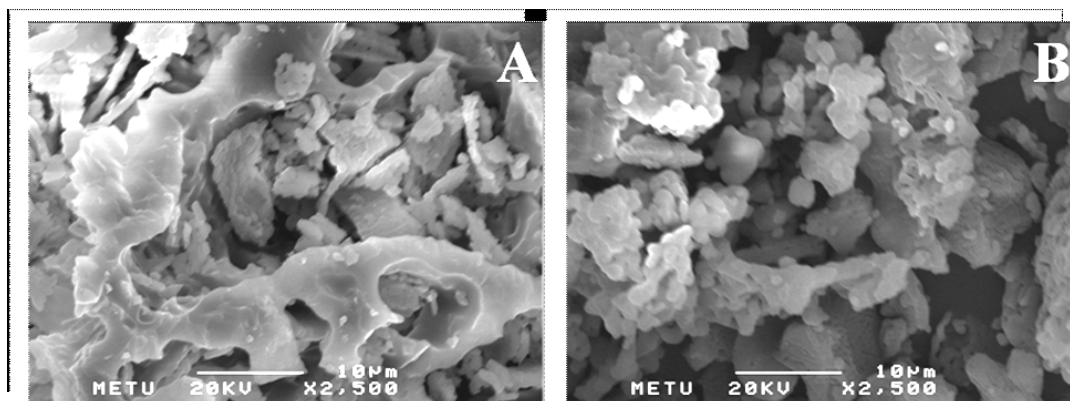


Figure 10: SEM images of wet synthesized undoped LTB (A) and solid synthesized undoped LTB (B).

Undoped wet synthesized and solid synthesized LTB samples have some morphological differences. Wet synthesized LTB has some melt or glassy structure without separate particle shapes, although solid synthesized LTB has different sized crystalline particles. (Figure 10) Particle size is not uniform according to SEM images of solid synthesized LTB.

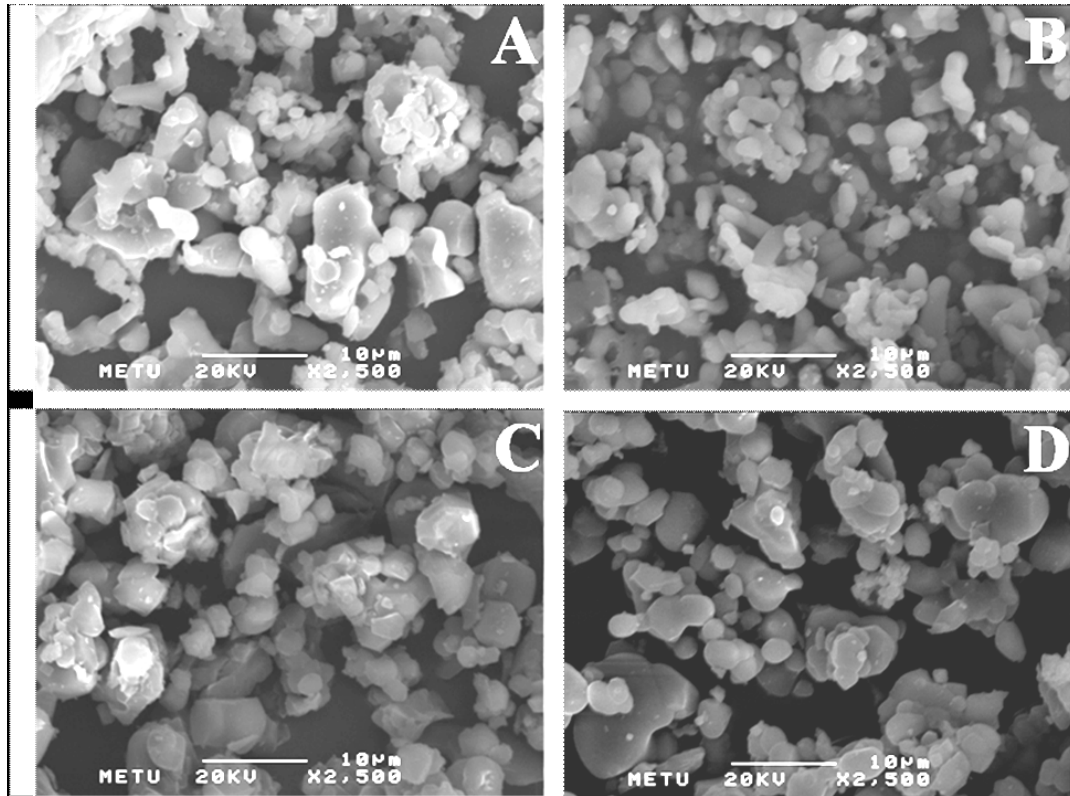


Figure 11: SEM images of wet synthesized 1 wt % Mn wet doped LTB (A), wet synthesized 1 wt % Mn solid doped LTB (B), solid synthesized 1 wt % Mn wet doped LTB (C), and solid synthesized 1 wt % Mn solid doped LTB (D).

Although SEM images are seem different from each other in wet and solid synthesized undoped LTB samples, after doping there are no more such morphological differences between four different types of doped products. Agglomeration of particles and varying particle size can be seen in all four images. (Figure 11)

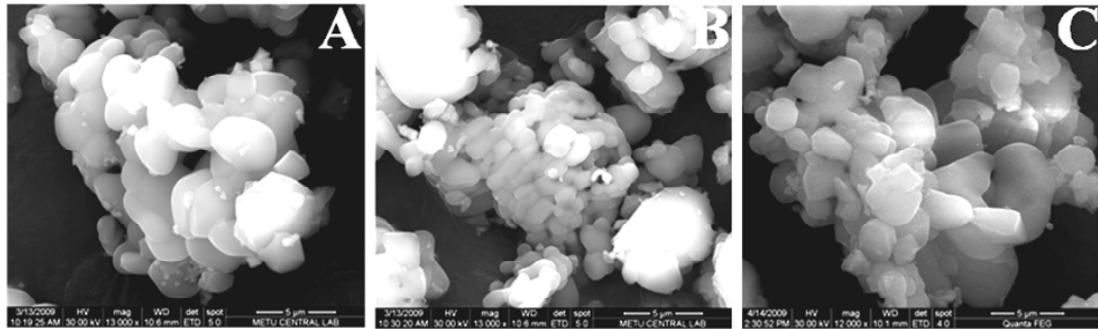


Figure 12: SEM images of solid synthesized 1 wt % Mn 0.5 wt % Ag solid doped LTB (A), solid synthesized 1 wt % Mn 0.5 wt % P solid doped LTB (B), and solid synthesized 1 wt % Mn 0.5 wt % Mg solid doped LTB (C).

In SEM images of Ag, P or Mg co-doped Mn doped LTB samples, still varying particle sizes and agglomeration of particles can be seen. Although there are serious differences in TL responses, morphologies compared from SEM images did not give reliable information about the reason of this difference for these samples.

3.1.5 Thermoluminescence Dosimetry (TLD)

TL glow curves of differently synthesized and differently doped and undoped samples of LTB were investigated.

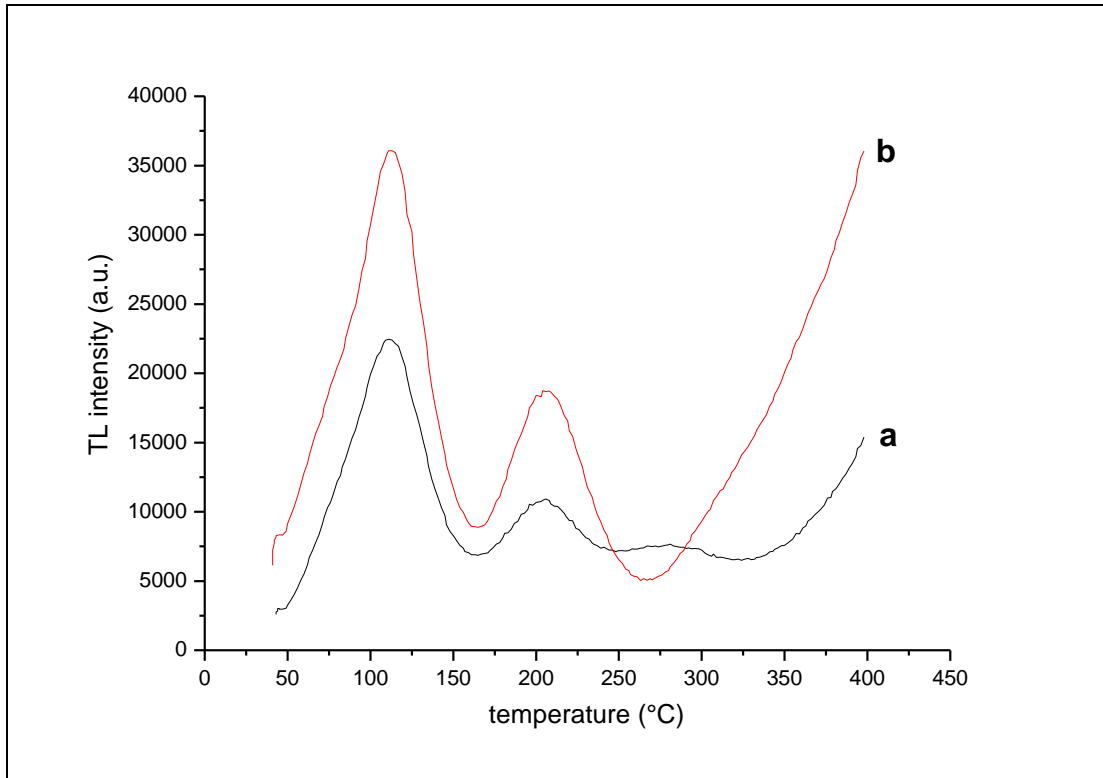


Figure 13: TL glow curves of undoped wet synthesized (a) and solid synthesized (b) LTB

In TL glow curves of undoped wet synthesized and solid synthesized LTB, it was possible to see two peaks and a background increase (Figure 13). In both samples, the first glow peak was present at about 110 °C and a lower intensity peak at about 200 °C, and a background increase was followed up to higher temperatures.

These glow curves were not in the desired form of a good glow curve described in literature as having a single sharp peak at the range of 180 °C and 250 °C. In order to enhance the glow curve properties and to investigate the effects of synthesis and doping methods on TL glow curves, LTB doped with varying Mn content by using different methods were analyzed on their glow curves.

Firstly the effect of increasing Mn content in LTB on glow curves was investigated in same synthesized and doped samples.

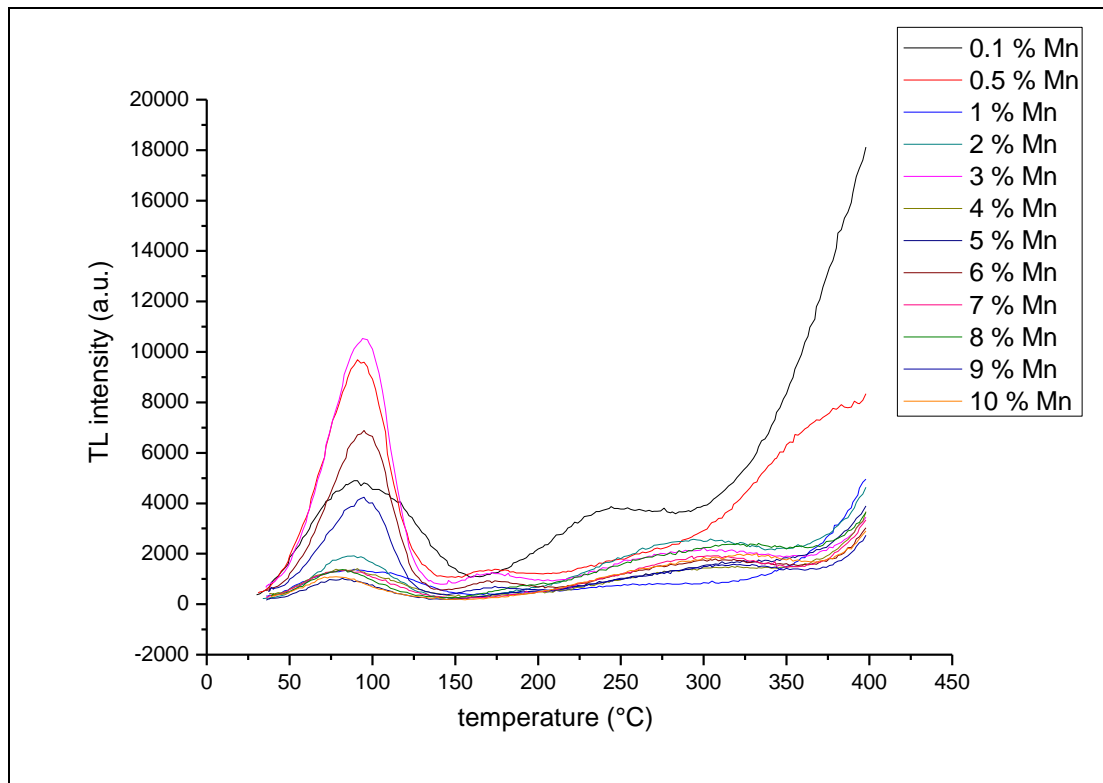


Figure 14: TL glow curves of wet synthesized and Mn doped by wet doping method with varying Mn content from 0.1 wt % to 10 wt %.

Wet synthesized and wet doped LTB:Mn samples with varying Mn content gave a glow curve consisting of one peak at about 100 °C and a shoulder like low intensity peak at about 250 °C and a final increase in background up to 400 °C and higher temperatures in TL measurements. The shape of the glow curve did not change in none of the compositions in the range of 0.1 wt % and 10 wt % Mn content in LTB. (Figure 14)

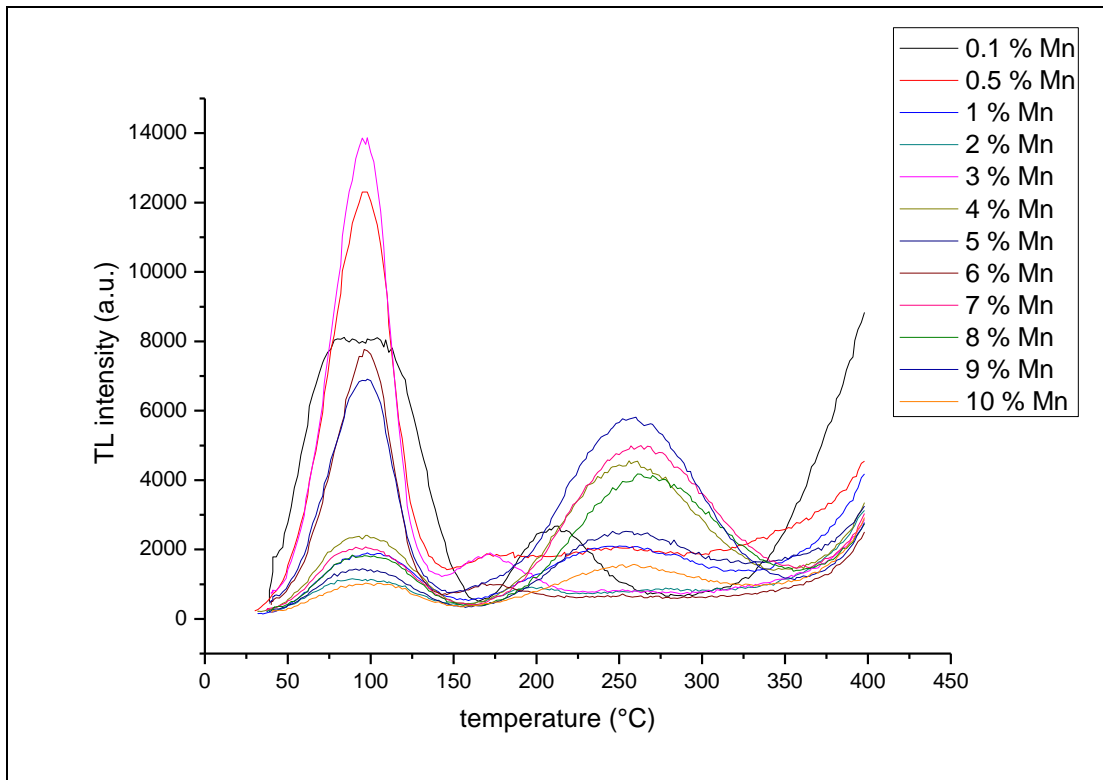


Figure 15: TL glow curves of wet synthesized and Mn doped by solid doping method with varying Mn content from 0.1 wt % to 10 wt %.

Wet synthesized and solid doped LTB:Mn samples had a similar glow curve with wet synthesized and wet doped samples with an small increase in 250 °C peak. Also in this set of varying Mn content, all of the compositions gave the same shape of glow curves. (Figure 15)

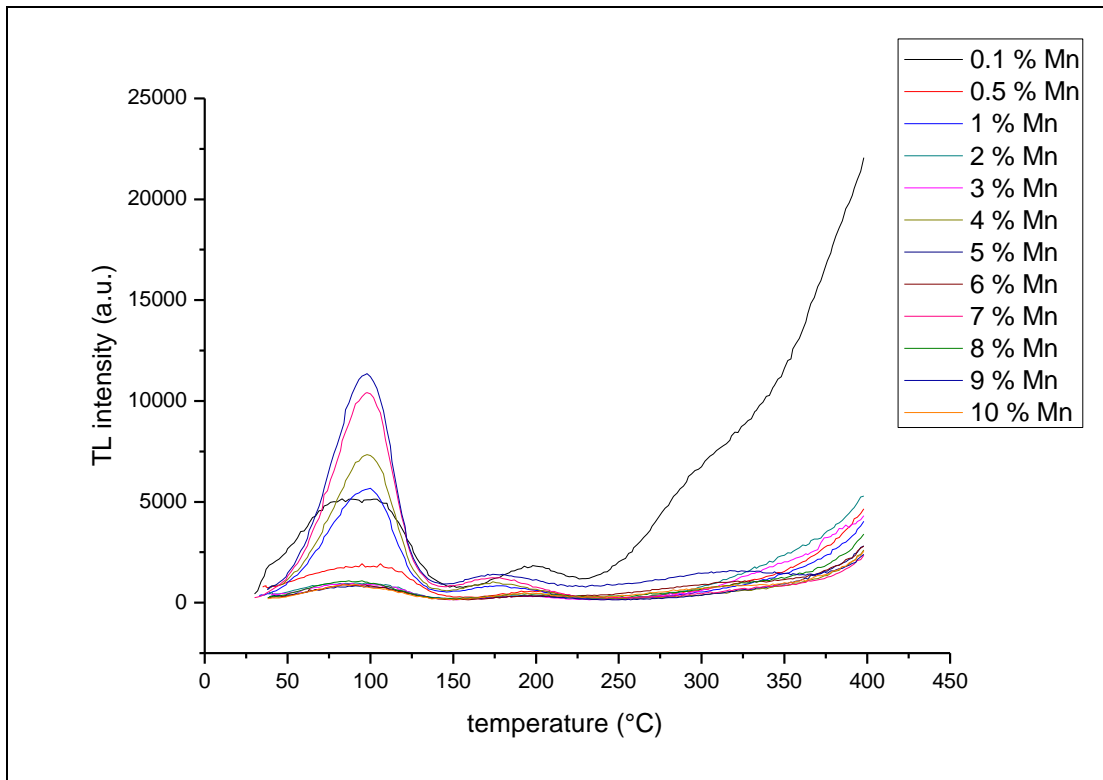


Figure 16: TL glow curves of solid synthesized and Mn doped by wet doping method with varying Mn content from 0.1 wt % to 10 wt %.

Solid synthesized and wet doped LTB:Mn samples had a peak at 100 °C and a lower intensity peak at about 180 °C. The intensity of 100 °C peak is 4 times higher than wet synthesized and wet doped samples, and also a similar background increase at very high temperatures was observed. (Figure 16)

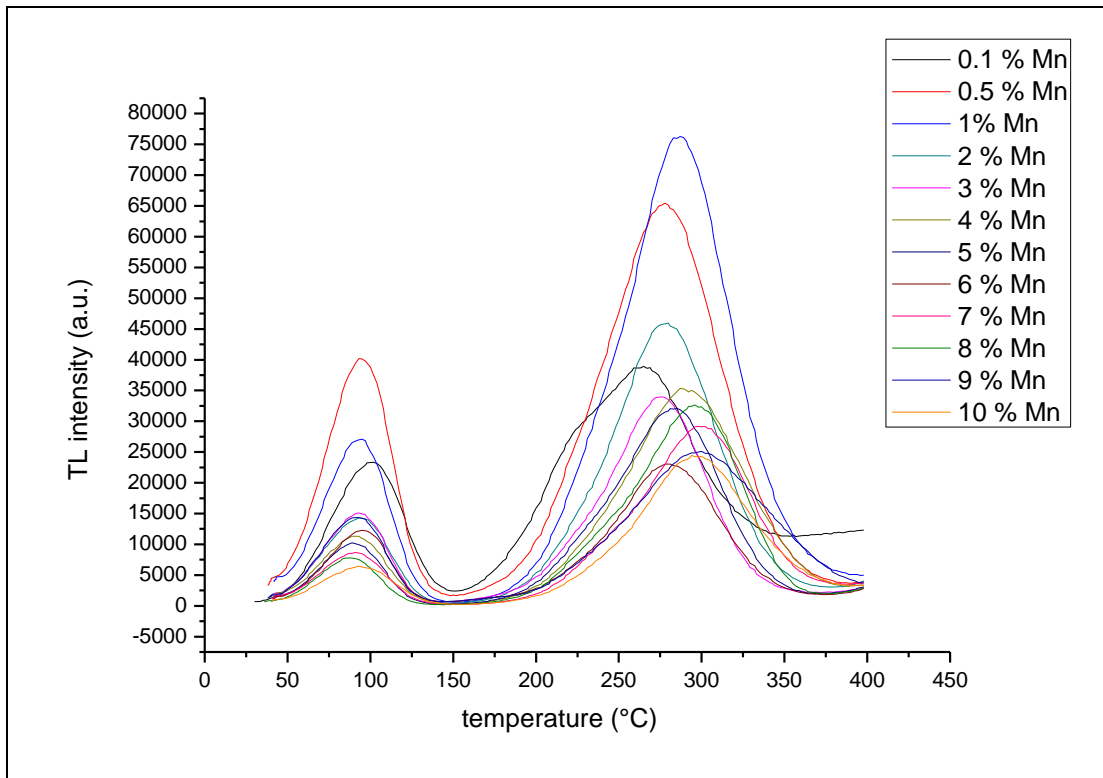


Figure 17: TL glow curves of solid synthesized and Mn doped by solid doping method with varying Mn content from 0.1 wt % to 10 wt %.

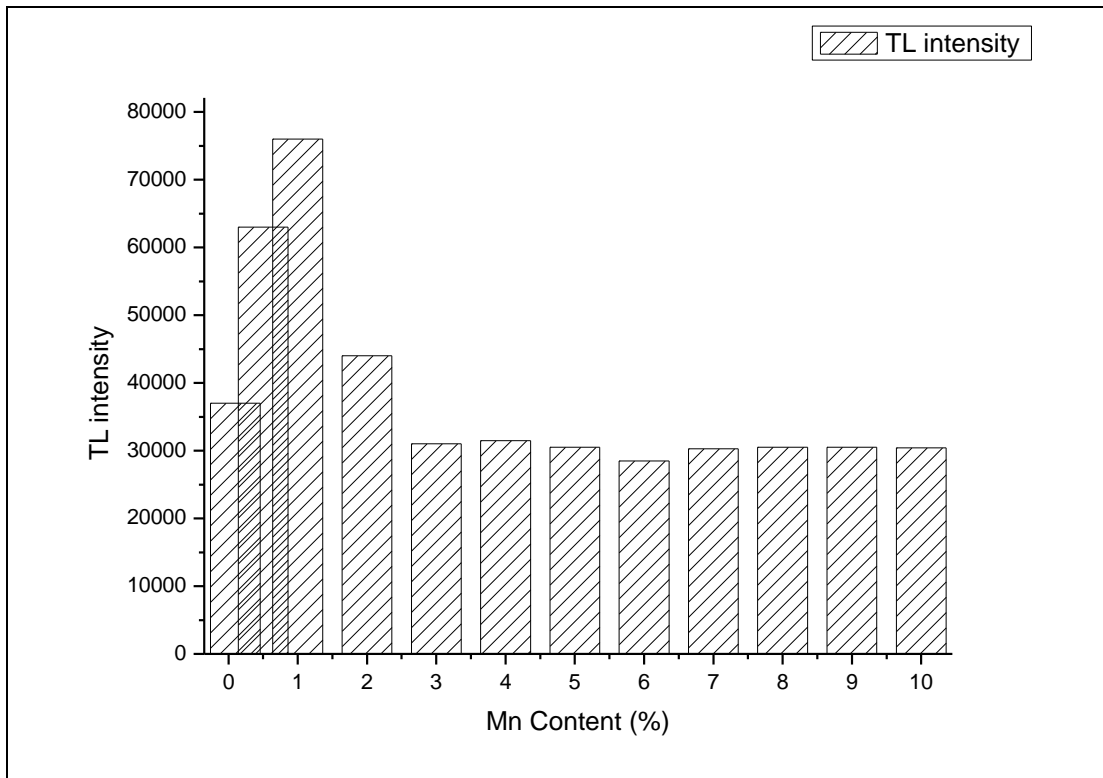


Figure 18: Glow peak intensities of solid synthesized and solid doped LTB with varying Mn content.

Solid synthesized and solid doped LTB:Mn samples gave a glow curve consisting of one peak at about 100 °C like the other 3 types of products. But this time there was a very high intensity peak at about 280 °C respectively. (Figure 17) Although the shape of the glow curve did not change in none of the compositions in the range of 0.1 wt % and 10 wt % Mn content in LTB, the intensity of the main glow peak at 280 °C is increasing in the order of 0.1 wt %, 0.5 wt % and 1 wt %. Above 1 wt % Mn in LTB, this intensity decreased with the increasing Mn content regularly.

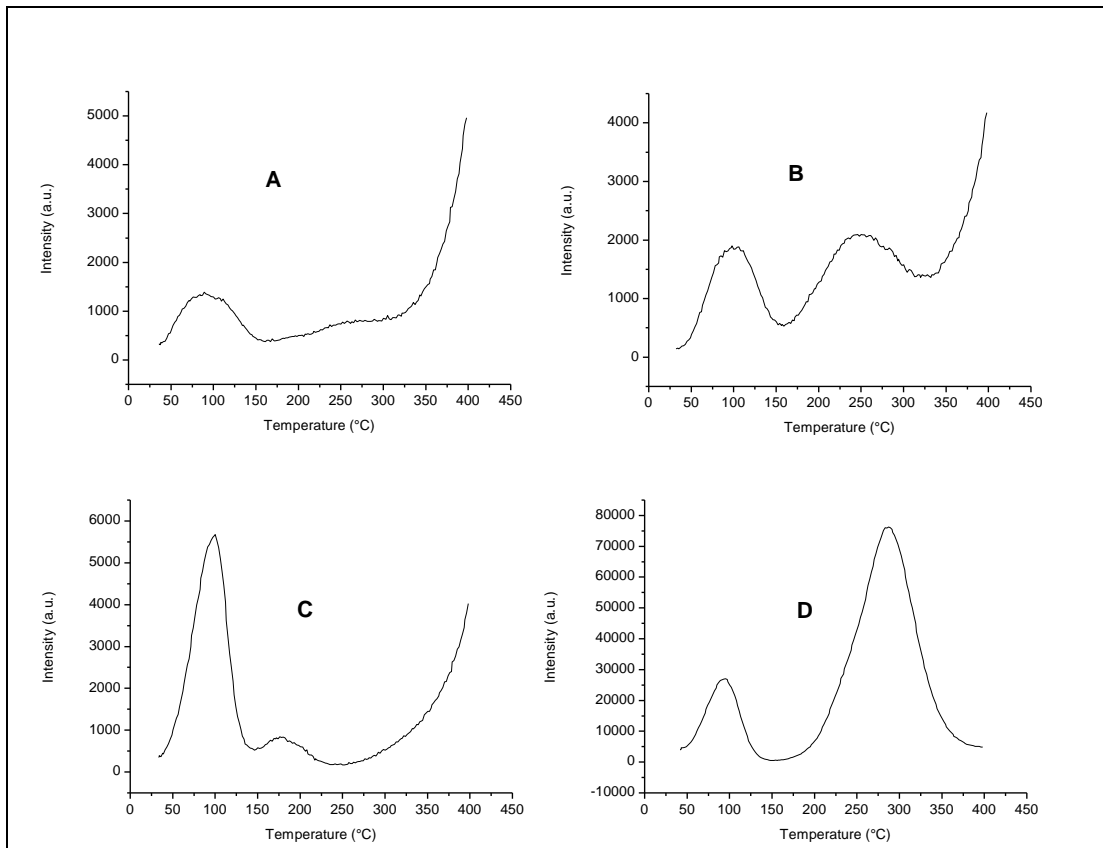


Figure 19: Thermoluminescence measurements of wet synthesized 1 wt % Mn wet doped LTB (A), wet synthesized 1 wt % Mn solid doped LTB (B), solid synthesized 1 wt % Mn wet doped LTB (C), and solid synthesized 1 wt % Mn solid doped LTB (D).

Glow peak temperature is important for dosimetric purposes and a good dosimetric material should give a glow curve consisting of a single sharp peak at the range of 180 °C and 250 °C, because peaks which are seen lower than 180 °C fade and disappear quickly at about 1 day, and peaks at higher temperatures than 250 °C the infrared emission from both TLD sample and the TLD holder may interfere (C. Furetta, C. 2003).

Since only solid synthesized and solid doped LTB:Mn samples gave a reasonably high intensity peak close to the usable temperature range, it is aimed to use these synthesis and doping methods to shift the peak at about 280 °C to the usable range by adding co-dopants such as Ag, P and Mg. For all co-dopants, the amount used is 0.5 wt % of LTB and Mn content varied between 0.1 wt % and 1 wt %.

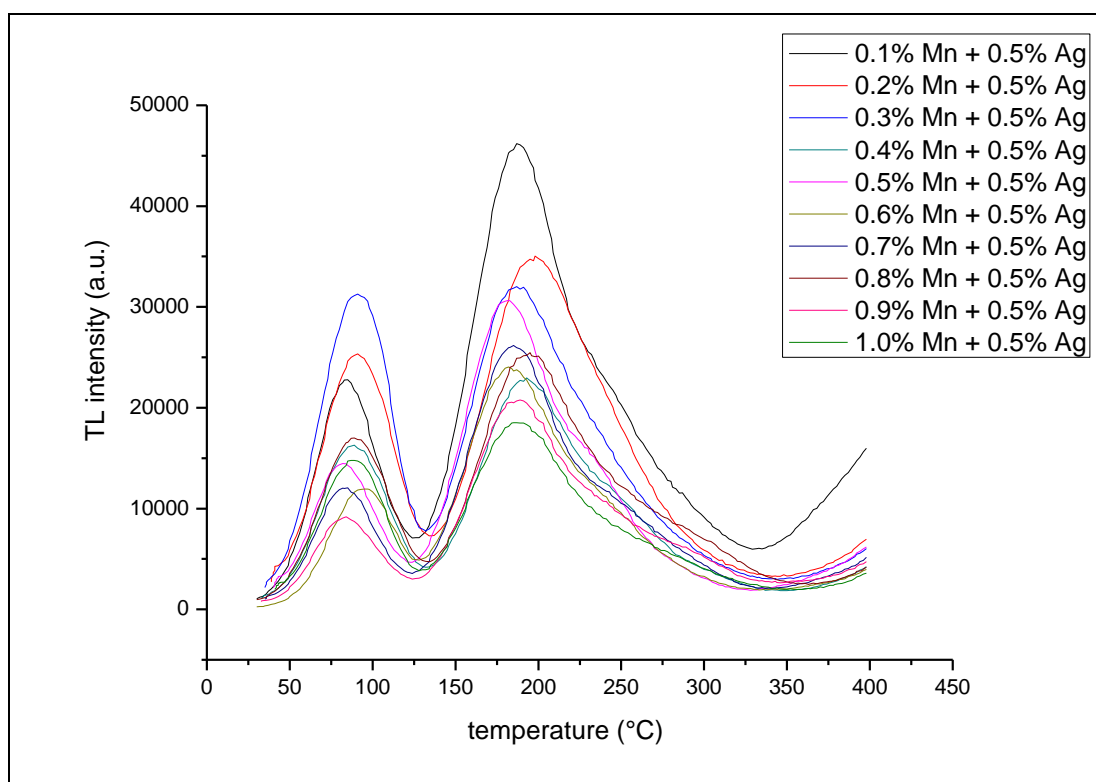


Figure 20: TL glow curves of solid synthesized and Mn and Ag doped by solid doping method with varying Mn content from 0.1 wt % to 1 wt % for Mn and 0.5 wt % for Ag.

Ag co-doped and Mn doped LTB gave a glow curve consisting of two peaks; one is at about 80 °C and a higher intensity peak at 200 °C. The best result with the highest intensity 200 °C peak, belongs to 0.1 wt % Mn and 0.5 wt % Ag content in LTB. (Figure 20)

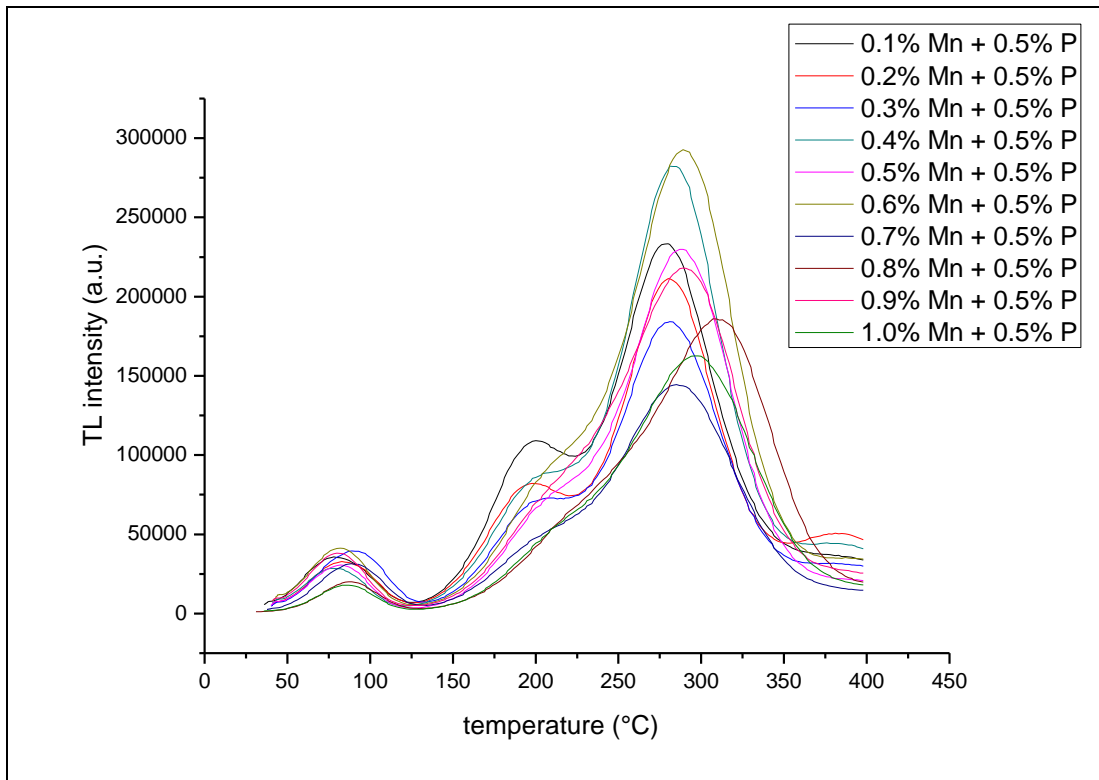


Figure 21: TL glow curves of solid synthesized and Mn and P doped by solid doping method with varying Mn content from 0.1 wt % to 1 wt % for Mn and 0.5 wt % for P.

Glow curve of P co-doped and Mn doped LTB has a peak at about 80 °C, another peak at about 200 °C and a higher intensity peak at 260 °C. Although the high temperature peaks in these samples have higher intensities than LTB:Mn,Ag samples, these results are not better than LTB:Mn,Ag results since complexity in glow curves is not preferable in those materials. (Figure 21)

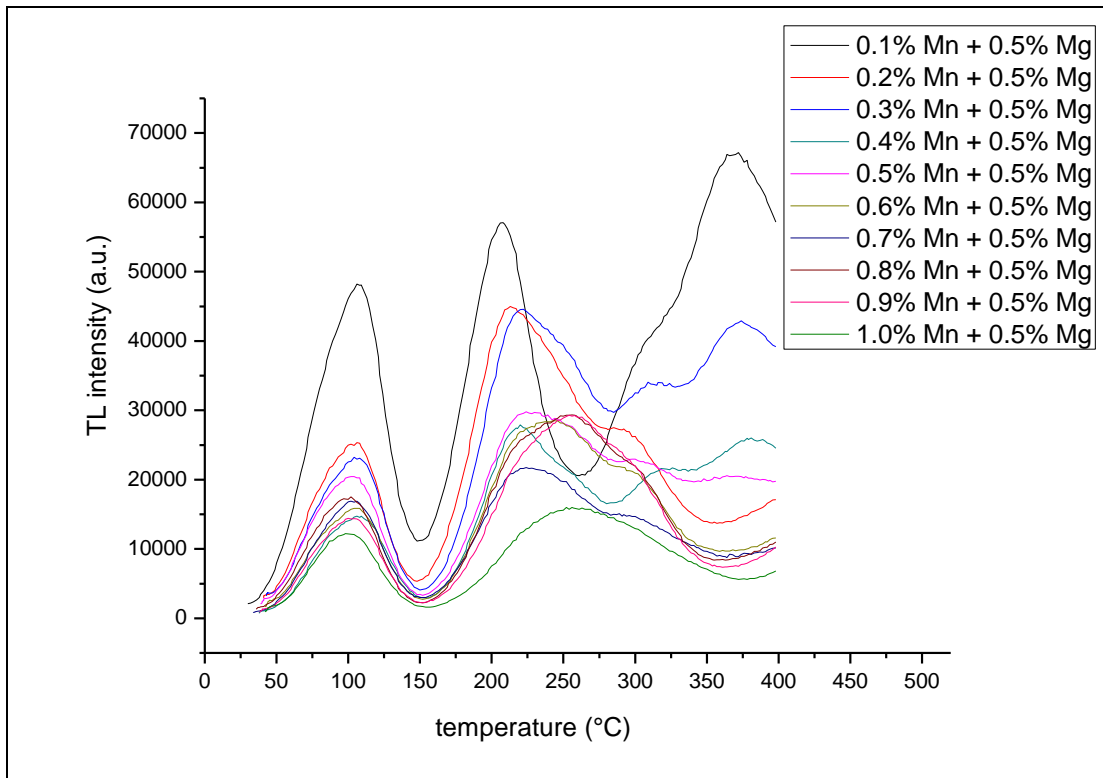


Figure 22: TL glow curves of solid synthesized and Mn and Mg doped by solid doping method with varying Mn content from 0.1 wt % to 1 wt % for Mn and 0.5 wt % for Mg.

Also Mg co-doped and Mn doped LTB samples gave a complex glow curve consisting of four peaks; one is at about 100 °C, one is at about 200 °C, a shoulder at about 300 °C and another peak at about 350 °C. (Figure 22)

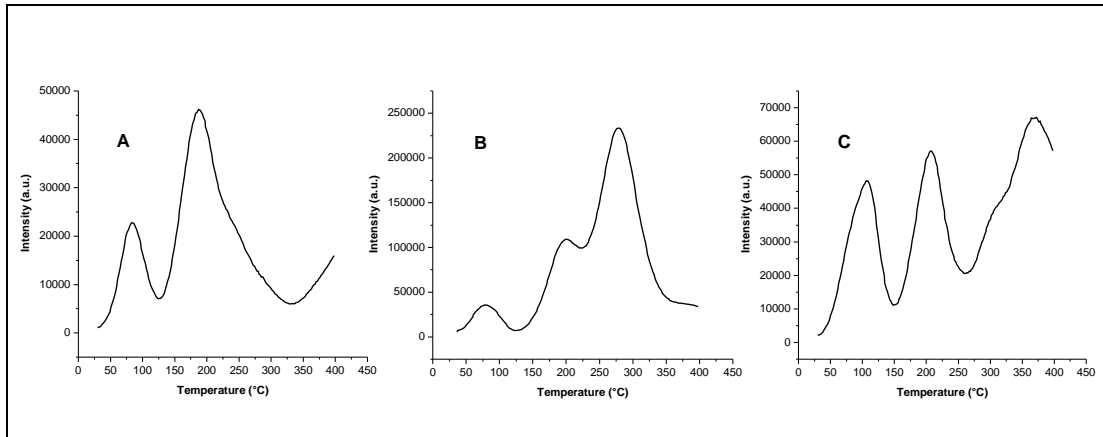


Figure 23: Thermoluminescence glow curves of LTB:Mn,Ag (A), LTB:Mn,P (B), and LTB:Mn,Mg (C).

In figure 23, it is possible to observe the changes in TL glow curves of Ag, Mg, or P co-doped system of LTB:Mn.

CHAPTER IV

CONCLUSIONS

LTB was synthesized by using two different methods; one was solid synthesis method and the other one was wet synthesis method. Both of the synthesis methods were successful to produce LTB.

XRD results revealed that both of the synthesis methods gave single phase polycrystalline LTB. XRD patterns of two differently synthesized products did not showed any difference in peak positions, peak intensities or peak shapes which indicates no structural differences. Also doped samples did not showed any structure deformation or impurity peaks.

FTIR results were in well agreement with XRD results, there were no structural differences between differently synthesized products and doped samples. There were no change in bonds between atoms, and there were no vibrations caused from any of the dopants used in this study.

ICP-OES results assured the concentrations of dopants, there was no loss of dopants during reaction.

Thermoluminescence glow curves of Mn doped LTB produced by using solid and wet synthesis methods and solid and wet doping techniques were investigated. Although there is no any morphological or structural differences between products of Mn doped LTB, thermoluminescence glow curves differs with synthesis and doping methods used.

Solid synthesis of LTB and solid doping of Mn gave better glow curves with 1 wt % Mn content than other products with different synthesis and doping methods and than other percentages of Mn in LTB.

The addition of Ag as co-dopant shifted the main glow peak to 200 °C. P increased the glow peak at 280 °C. Mg increased the glow curve complexity.

CHAPTER V

REFERENCES

A. C. Fernandes, M. Osvay, J. P. Santos, V. Holovey, M. Ignatovych, *Radiation Measurements* 43 (2008) 476 - 479.

A. Davydov, *Molecular Spectroscopy of Oxide Catalyst Surfaces*, University of Alberta, Edmonton, Canada, Syntroleum Corporation, Tulsa, Oklahoma, USA, Wiley 2003

A. Kelemen, V. Holovey, M. Ignatovych, *Radiation Measurements* 43 (2008) 375-378

A. S. Pradhan, *Radiation Protection Dosimetry*, 1 (3), 153-167, 1981

A. T. Ege, E. Ekdal, T. Karali, N. Can, *Radiation Measurements*, 42, 1280-1284, 2007

A. T. Ege, E. Ekdal, T. Karali, N. Can, M. Prokic, *Meas. Sci. Technol.* 18 (2007) 889–892

B. Andıçođlu, Ms. Thesis, 2005, METU

B. F. Wall, C. M. H. Driscoll, J. C. Strong, E. S. Fisher, *Phys. Med. Biol.* 27 (1982) 1023-1034

B. M. Hunda, V. M. Holovey, I. I. Turok, A. M. Solomon, P. P. Puga, G. D. Puga, *Inorganic Materials* 41-9 (2005) 990-994

C. Furetta, *Handbook of Thermoluminescence*. New Jersey, London, Singapore, Hong Kong: World Scientific, 2003.

C. M. H. Driscoll, E. S. Fisher, C. Furetta, R. Padovani, D. J. Richards, B. F. Wall, *Radiation Protection Dosimetry* 6 (1983) 305-308

E. Pekpak, Ms. Thesis, 2009, METU

G. Busuoli in *Applied Thermoluminescence Dosimetry, ISPRA Courses*, Edited by M. Oberhofer and A. Scharmann, Adam Hilger publisher (1981)

G. Corradi, V. Nagirnyi, A. Kotlov, A. Watterich, M. Kirm, K. Polgár, A. Hofstaetter M. Meyer, *J. Phys.: Condens. Matter* 20 (2008) 025216 (9pp)

G. Kitis, C. Furetta, M. Prokic, V. Prokic, *J. Phys. D: Appl. Phys.* 33 (2000) 1252-1262

J. Azorin, *International Journal of Radiat. Appl. Instrum. Part D Nucl. Tracks*, 11 (3), 159-166, 1986

JCPDS card supplied by ICDD, card no 18-0717

JCPDS card supplied by ICDD, card no 70-0735

JCPDS card supplied by ICDD, card no 47-0339

J. D. Henry, M. C. Weinberg, D. R. Uhlmann, *Journal of Materials Science* 33 (1998) 3853 – 3858

J. Krogh-Moe, *Acta Crystallogr.* 15 (1962) 190

Kang-Soo Park, J. K. Ahn, D. J. Kim, H. K. Kim, Y. H. Hwang, D. S. Kim, M. H. Park, Yumi Park, Jin-Joo Yoon, Jae-Young Leem, *Journal of Crystal Growth* 249 (2003) 483-486

M. D. Mathews, A.K. Tyagi, P.N. Moorthy *Thermochimica Acta* 320 (1998) 89-95

M. Ishii, Y. Kuwano, S. Asaba, T. Asai, M. Kawamura, N. Senguttuvan, T. Hayashi, M. Koboyashi, M. Nikl, S. Hosoya, K. Sakai, T. Adachi, T. Oku, H. M. Shimizu, *Radiation Measurements* 38 (2004) 571 – 574

M. J. Aitken, *Thermoluminescence Dating*, Academic Press, London (1985) – Standard text for introduction to the field. Quite complete and rather technical, but well written and well organized. There is a second edition.

M. J. Aitken, *Introduction to Optical Dating*, Oxford University Press (1998) – Good introduction to the field.

R. Chen, S. W. S. McKeever, *Theory of thermoluminescence and Related Phenomena*, World Scientific (1997)

R. Chen, Y. Kirsh, *Analysis of Thermally Stimulated Processes*, Pergamon Press (1981)

R. Grün Electron spin resonance dating. In Taylor RE and Aitken MJ (eds) Chronometric and Allied Dating in Archaeology. Plenum: New York (1997) 217-61

Sangeeta, Babita Tiwari, S.C. Sabharwal Journal of Crystal Growth 273 (2004) 167–171

S. G. Gorbics, A.E. Nash, F.H. Attix, Proc. 2nd Int. Conf on Lum. Dos., Gatlinburg, TN, USA, 587 (1968)

S. Lorrain, J.P. David, R. Visocekas, G. Marinello, Radiation Protection Dosimetry 17 (1986) 385-392

S. W. S. McKeever, Thermoluminescence of Solids, Cambridge University Press (1985)

T. Depçi, Phd. Thesis, 2009, METU

T. Sugawara, R. Komatsu, S. Uda, Journal of Crystal Growth 193 (1998) 364-369

The Australian National University, Trapped Charge Dating (ESR, TL, OSL), http://rse.anu.edu.au/research/ee/resources/index.php?p=trapped_charge (2007)

V. M. Holovey, V. I. Sidey, V. I. Lyamayev, M. M. Birov, Journal of Physics and Chemistry of Solids 68 (2007) 1305-1310

W. T. Reburn, W. A. Gale, J. Phys. Chem. 59 (1955) 19

Wikimedia Foundation Inc., Czochralski process, http://en.wikipedia.org/wiki/Czochralski_process (2009)

Wikimedia Foundation Inc., Bridgman Stockbarger technique,
http://en.wikipedia.org/wiki/Bridgman-Stockbarger_technique (2009)

Z. Keizars, 2008b. NRTL trends observed in the sands of St. Joseph Peninsula, Florida. Queen's University. Presentation: Queen's University, Kingston, Ontario, Canada.

Z. Özdemir, Phd. Thesis, 2006, METU